Extended X-ray Absorption Fine Structure Studies of Amorphous and Crystalline Si-Ge Alloys with Synchrotron Radiation

(Received May 20, 1988)

Hiroshi KAJIYAMA

Advanced Research Laboratory, Hitachi, Ltd., Kokubunji, Tokyo 185

ABSTRACT

Extended X-ray absorption fine structure (EXAFS) has been developed to a useful tool for determining the local bonding structure around an X-ray absorbing atom. EXAFS spectra are usually interpreted by a simple formula derived from an electron scattering theory, with the plane wave approximation. A curve-fitting technique gives plausible bond lengths, where the absorbing edge energy, E_0, is used as one of the parameters. Model compounds are necessary to get the reliable structure in most cases. However, in the case of binary or ternary compounds, it is unreasonable to yield different values of E_0 for different neighboring atoms through the curve-fitting procedure. Furthermore, it is difficult to find good model compounds.

A new method has been developed here for the EXAFS analysis, which is based on the spherical wave approach for emitted electrons. This method is proved to give a reliable structure even without model compounds. Ge K-edge EXAFS spectra have been measured for amorphous-$Si_{1-x}Ge_x$:H (x=0.27, 0.36, 0.38, 0.47, 0.56, 1.0) and crystalline-$Si_{1-x}Ge_x$ (x= 0.2, 0.39, 0.59 , 0.81, 1.0), using synchrotron radiation as the photon source. Spectra were analyzed by the newly developed method without using model compounds and by fixing the E_0 value at the steepest point of the absorption edge.

Obtained results show that Ge-Ge and Ge-Si bond lengths of amorphous- $Si_{1-x}Ge_x$:H are 2.46Å and 2.41Å, respectively, irrespective of Ge concentration. These bond lengths can be interpreted by the sum of the atomic radii of constituent

elements as pointed by Bragg and later by Pauling. As for the case of crystalline-$Si_{1-x}Ge_x$, the resulted bond lengths of Ge-Ge and Ge-Si were almost similar to the corresponding bond lengths in amorphous-$Si_{1-x}Ge_x$:H. The difference of crystalline and amorphous alloys should be only interpreted by the difference of bond angle distortion. A study on the coordination around a Ge atom in amorphous-$Si_{1-x}Ge_x$:H revealed that Ge and Si atoms are randomly mixed in the compositional range below 40 atomic percent. In the amorphous alloys with higher Ge content, the coordinations of Ge atoms surrounding a central Ge atoms is 15-20 percent higher than expected for a random mixture, suggesting a structural inhomogeneity in Ge-rich region. Whereas in crystalline $Si_{1-x}Ge_x$, it is found that Ge and Si atoms are randomly mixed in the studied compositional range.

CONTENTS

1. Introduction

2. Experimental procedures

2.1 Sample preparation

2.2 Measurement

2.3 Data processing

3. EXAFS analysis without using model compounds

3.1 Computational procedures

3.2 Plane wave analysis

3.3 Spherical wave analysis

3.3 Absorption edge energy problem

4. Discussion

4.1 Hydrogenated amorphous Silicon-Germanium alloys ($a-Si_{1-x}Ge_x:H$)

4.2 Crystalline Silicon-Germanium alloys ($c-Si_{1-x}Ge_x$)

5. Conclusion

6. Acknowledgement

7. References

1. INTRODUCTION

X-rays photons are absorbed by an atom, followed by the ejection of a core electron. The scattering of the ejected photoelectrons by neighboring atoms causes the interference of this reflected electron wave with the outgoing photoelectron waves, leading to modulation of the X-ray absorption cross section.

Such modulation is observed as the fine structure in X-ray absorption spectrum, starting from about 100 eV and extending to about 1000 eV above an absorption edge, which is called 'extended X-ray absorption fine structure' (EXAFS).[1,2] Accordingly, EXAFS spectra involve the structural information around an X-ray absorbing atom. EXAFS as a technique of structural analysis has been developed remarkably in recent years mainly due to two reasons. First is the advent of synchrotron radiation,[3] whose use as the X-ray source makes it possible to measure EXAFS in much shorter time than the case of the conventional X-ray source, with high signal to noise ratio. Second is the establishment of theoretical analysis of EXAFS spectra. Stern and Sayers[4] have derived a simple formula for an EXAFS oscillation with several drastic but reasonable assumptions, and obtained the radial distribution function of a specific atom of interest through the Fourier analysis.

In fact, the Fourier method is convenient to grasp an outline about surrounding atoms. It is however not enough to give any reliable structural information, such as bond distances and coordination numbers. A curve fitting method has been

exploited, where the theoretical EXAFS oscillation calculated from the above simple formula is adjusted to the experimental one until we get the best fit between them with appropriate parameters. In the curve-fitting analyses [5-7], the interatomic distance, number of atoms and the Debye-Waller factor for each coordination shell are the fitting parameters. Sometimes the absorption edge energy, E_0, is also treated as a fitting parameter to obtain the best fit. Significant progress in the accuracy of this method has been achieved with the fine adjustment technique based on model compound (FABM) technique.[7] This FABM technique works well, provided that suitable model compounds with well-known structure are available. The crystal structure of a sample compound can be estimated reliably if the correlation between the E_0 and interatomic distance, R, of the sample is same as that of the model compound. It should be noted that such compounds cannot always be available: We cannot find any good model compounds for silicon-germanium alloys, in which Si and Ge atoms form a liquid solution throughout the entire compositional range.

Although the FABM technique is excellent for analyzing multi-shell contributions with high accuracy, its physical basis is obscure. An optimum E_0 inevitably results in different values for the individual bonds in the FABM technique. It is noteworthy that the E_0 value is by no means an adjusting parameter and must have the same value for individual bonds.

It is really necessary to establish a physically reasonable method for EXAFS analysis. The primary purpose of this study is to show that EXAFS oscillation caused by two coordination shells

can be analyzed with the same E_0 value for each bond, and that a newly developed formula, which is based on the spherical wave approach for emitted photoelectrons, does not need any model compounds.

This new technique of EXAFS analysis has been applied for the first time to the silicon-germanium alloys: hydrogenated amorphous alloys (a-$Si_{1-x}Ge_x$:H) and crystalline alloys (c-$Si_{1-x}Ge_x$).

In chapter 2, experimental procedures are described. In chapter 3, experimental EXAFS spectra for a-$Si_{1-x}Ge_x$:H have been analyzed using the EXAFS formula based on plane wave approximation and spherical wave approximation. The absorption edge energy problem in the curve- fitting analysis has also been discussed. In chapter 4, experimental EXAFS for a-$Si_{1-x}Ge_x$:H and c-$Si_{1-x}Ge_x$ have been analyzed using the EXAFS formula based on the spherical wave approximation. The bond lengths for Ge-Ge, Ge-Si, and coordinations on the nearest sites for Ge and Si atoms have been evaluated.

2. EXPERIMENTAL PROCEDURES

2.1 Sample preparation

A: Amorphous Silicon-Germanium alloys (a-$Si_{1-x}Ge_x$:H)

Samples were prepared by rf glow discharge decomposition of disilane (Si_2H_6) and germane (GeH_4) mixtures in a capacitively coupled diode system.[8] Each film was grown at a deposition rate of 3-7Å/s to the thickness ranging from 0.6 to 2 µm on a 25 µm-thick polyimide film. The temperature of the substrate was 230 C and the pressure was 0.45 torr during the reaction. The rf power density was held constant at 0.65 W/cm^2

The Ge concentration in the films was varied by adjusting the flow rates of Si_2H_6 and 21% GeH_4 diluted with H_2, keeping the total gas flow rate constant at 20 cm^3 STP per minute(SCCM). The chemical composition was determined by inductively coupled argon plasma atomic-emission spectroscopy. Several kinds of a-$Si_{1-x}Ge_x$:H were prepared with different Ge concentration; x=0.27, 0.36, 0.38, 0.47, 0.56, 1.0. To prevent oxygen from being incorporated into the films, all samples were kept in a nitrogen atmosphere before the measurements.

B: Crystalline Silicon-Germanium alloys (c-$Si_{1-x}Ge_x$)

Samples were prepared by rf glow discharge decomposition of disilane (Si_2H_6) and germane (GeH_4) mixtures in a capacitively coupled diode system.[8] The films were grown at a deposition rate of 4.3-13.5 Å/s to the thickness ranging from 0.77 to 2.43 µm on 0.8mm-thick polycrystalline graphite substrates. The temperature of the substrate was 300 C and the pressure was 0.45

torr during the reaction. The rf power density was held constant at 0.65 W/cm^2. All samples were annealed at 700°C for 5h in argon atmosphere and cooled down gradually. The crystallization was confirmed by the x-ray diffraction measurement.

The Ge concentration in the film was varied by adjusting the flow rate of Si_2H_6 and 21 % GeH_4 diluted with H_2, keeping the total gas flow rate constant at $20cm^2$ at STP per minute(SCCM). The chemical composition was determined by inducting coupled argon plasma atomic-emission spectroscopy. Several kinds of $Si_{1-x}Ge_x$ films were prepared with different Ge concentration; x=0.19, 0.39, 0.59, 0.81, 1.0.

2.2 Measurements

The EXAFS measurements were carried out at the EXAFS station (either Beam line 10B or 8C)[9,10] of the Photon Factory at the National Laboratory for High Energy Physics in Tsukuba, Japan. Figure 1 shows a schematic diagram of EXAFS measurement at the beam line 10B and/or 8C. The electron storage ring was operated at 2.5 Gev. During the measurements in 10B and 8C stations, the beam current ranged from 60 to 145 mA and from 140 to 260 mA, respectively.

The X-ray absorption spectra were taken on the K-edge of Ge, using a monochromator. At the beam line 10B and 8C, the monochromator is equipped with a Si(311) channel-cut crystal and a Si(111) double-crystal, respectively. The absorption measurements were performed in the transmission mode at room temperature. To obtain the optimum sample thickness for

absoprtion measurements, several tens of the same sample film were stacked. The incident and transmitted x-ray intensities, I_0 and I respectively, were monitored simultaneously with two ionization chambers. Here, $\ln(I_0/I)$ is equal to ut, where u is the linear absoprtion coefficient and t the absorber thickness. The measured energy range was from 500eV below to 1000eV above the absorption edge. The enegy resolution was estimated to be 1-2 eV.

2.3 Data processing

Photoelectrons ejected from x-ray absorbing atoms can be characterized by the photoelectron wave number k, which is given by

$$k = \sqrt{\frac{2m}{\hbar^2}(h\nu - E_0)} \tag{1}$$

where m is the electron mass, $h\nu$ is the incident photon energy and E_0 is the absorption edge energy. In the present analysis, the energy for Ge-K edge was defined as the steepest point of the edge jump on the experimental absorption coefficient vs. photon energy curve.[11] The normalized EXAFS oscillation, $\chi(k)$, is defined as a function of k as follows:

$$\chi(k) = (\mu(k) - \mu_0(k)) / \mu_0(k) \tag{2}$$

,where $\mu(k)$ and $\mu_0(k)$ are the K-shell absorption coefficient for the atoms in its environment and for the isolated atom, respectively.

EXAFS oscillations were obtained in the conventional manner.[12] The first step is the subtraction of the background

above the absorption edge, since the measured spectra often contain both EXAFS signals and background. To estimate the background function, the pre-edge spectrum was first fitted with a quadratic function of wave length and then extrapolated to above the absorptin edge. Next, the above-edge background function, μ_0, was generated by the cubic-spline technique. Subtraction of the background function yields the EXAFS signal.

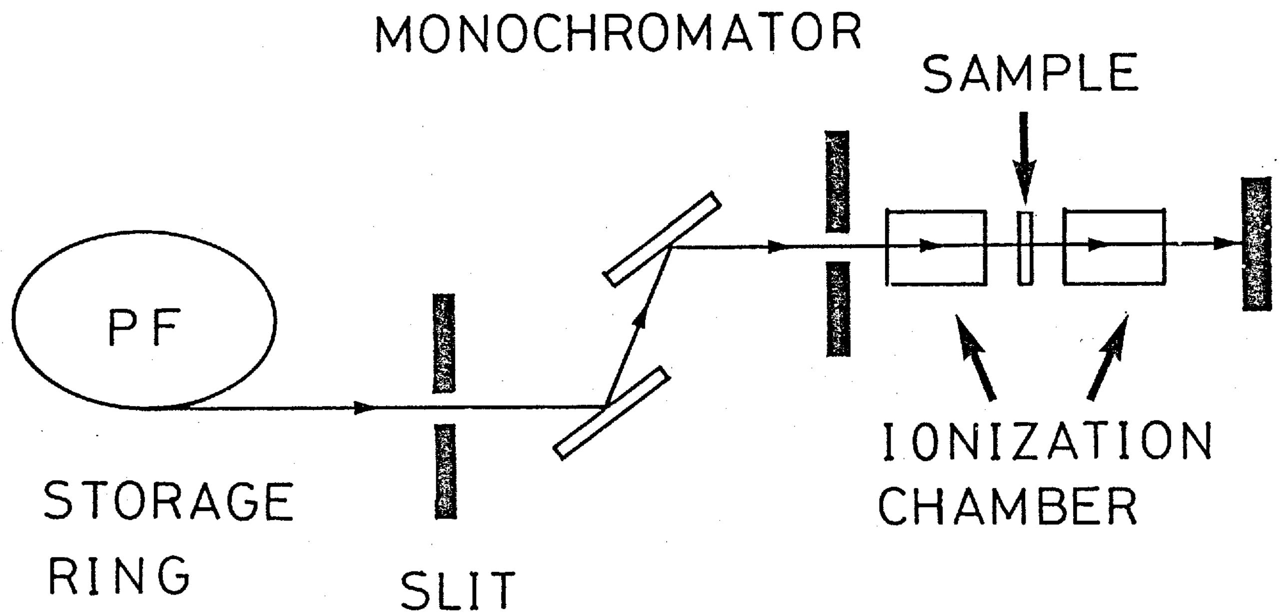

Fig.1 Schematic diagram of EXAFS measurement at the beam line 10B and 8C of Photon Factory. Intensities of incident and transmitted X-rays are measured by two ionization chambers.

3. EXAFS ANALYSIS WITHOUT USING MODEL COMPOUNDS

3.1 Computational procedures

Some formulae based on spherical waves for a single scattering process have been independently developed.[13-15] The K-edge EXAFS, $\chi(k)$, for non-polarized X-rays in a single scattering process is described by the following final expression,[15]

$$\chi(k) = -\mathrm{Im}\left[\sum_{j\neq 0,l} (2l+1)\exp(2i\delta_1^0 + i\delta_l^j)\sin(\delta_l^j) \times \left\{ l(l+1)\left[h_l^{(1)}(\rho_j)/\rho_j\right]^2 + \left[l\, h_l^{(1)}(\rho_j)/\rho_j - h_{l+1}^{(1)}(\rho_j)\right]^2\right\}\right] \quad (3)$$

where ρ_j is given by $\rho_j = k\, r_j$ with r_j the distance of the j-th scattering atom from the absorbing atom. The δ_l^j is the p-wave phase-shift of the photoelectron at the absorbing atom, δ_1^0 is the phase shift of the l-th partial wave at the j-th scattering atoms and $h_l^{(1)}(\rho)$ is the first kind spherical Hankel function of order l. If we take only the first term in the following asymptotic expansion for $\rho \rightarrow \infty$,

$$h_l^{(1)}(\rho) \simeq (-i)^{l+1}\frac{e^{i\rho}}{\rho}\left[1 + i\frac{l\,(l+1)}{2\rho} + \cdots\right] \quad (4)$$

the l-summation in Eq.(3) can be expressed with the backscattering amplitude $f_j(\pi)$:

$$\chi(k) \simeq -\mathrm{Im}\left[\sum_{j\neq 0} f_j(\pi)\,(2l+1)\exp\left[2i\,(\delta_1^0 + kr_j)\right] / kr_j^2\right] \quad (5)$$

This asymptotic equation corresponds just to a conventional formula.[3,16]

The physical quantities used to calculate Eq.(3) and Eq.(5)

were obtained as follows. The phase shifts of the photoelectron at the absorbing atom were taken from the numerical tables given by Teo and Lee[17] with Herman and Skillman wave functions.[18] Figure 2 shows central atom phase shift of germanium atom. The phase shifts for the scattering atom (l = 0 - 12) were calculated with a program developed by Pendry[11] from core state wave functions.[18] The phase shifts due to electron scattering by silicon and germanium are shown in Fig. 3 and Fig. 4, respectively. The effect of thermal vibration of scattering atoms was included in the thermal Debye parameter, B.[15] The B factor at room temperature , $\overline{B_{293}}$, was estimated to be 0.30 and 0.31 $\mathring{A}^2$ for Ge and Si atoms, respectively, from the characteristic Debye temperature for the crystal of each element.[20,21] The absolute value of backscattering amplitude for silicon and germanium atoms at B=0.0 are shown in Fig. 5. The absolute value of backscattering amplitude of vibrating silicon and germanium atoms at room temperature are shown in Fig. 6. The effect of inelastic scattering of photoelectrons was included in a form, $\exp(-\frac{2r_j}{\lambda})$, where r_j is the interatomic path-length and λ is the mean free path. As the mean free path, the escape depth of crystalline germanium was adopted, which was measured by Gant and Monch [22], and is shown in Fig. 7.

The normalized EXAFS oscillations, $\chi(k)$, were analyzed by the fine-adjustment technique without the use of model compounds. In brief, the calculated EXAFS oscillation based on the above described formulae[3,15,16] were adjusted to the experimental ones.

The best-fit between the experimental and the theoretical

EXAFS oscillations was obtained by adjustng four fitting parameters; Ge-Ge and Ge-Si bond lengths and coordination ratios of Ge and Si atoms surrounding Ge atoms. Here, the coordination ratio is defined as the number of Ge or Si atoms (N_{Ge}, N_{Si}) devided by the total coordination number of Ge and Si atoms ($N_{Ge} + N_{Si}$) surrounding Ge atoms; for example, the Ge coordination ratio is equal to $N_{Ge}/(N_{Ge} + N_{Si})$. The coordination ratio was employed because the total coordination number around Ge atoms cannot be determined definitely in a-$Si_{1-x}Ge_x$:H films in which H atoms are also bonded to Ge and Si atoms.[23] Backscattering from H atoms is not observable in EXAFS. It should be noted that the coordination ratio thus determined is not affected by the content of H atoms bonded to Ge and Si atoms even if the H content in the films changes with the Ge concentration. In the fitting procedure, the bond lengths and the coordination ratios of Ge and Si atoms were by 0.005 Å and 0.05, respectively.

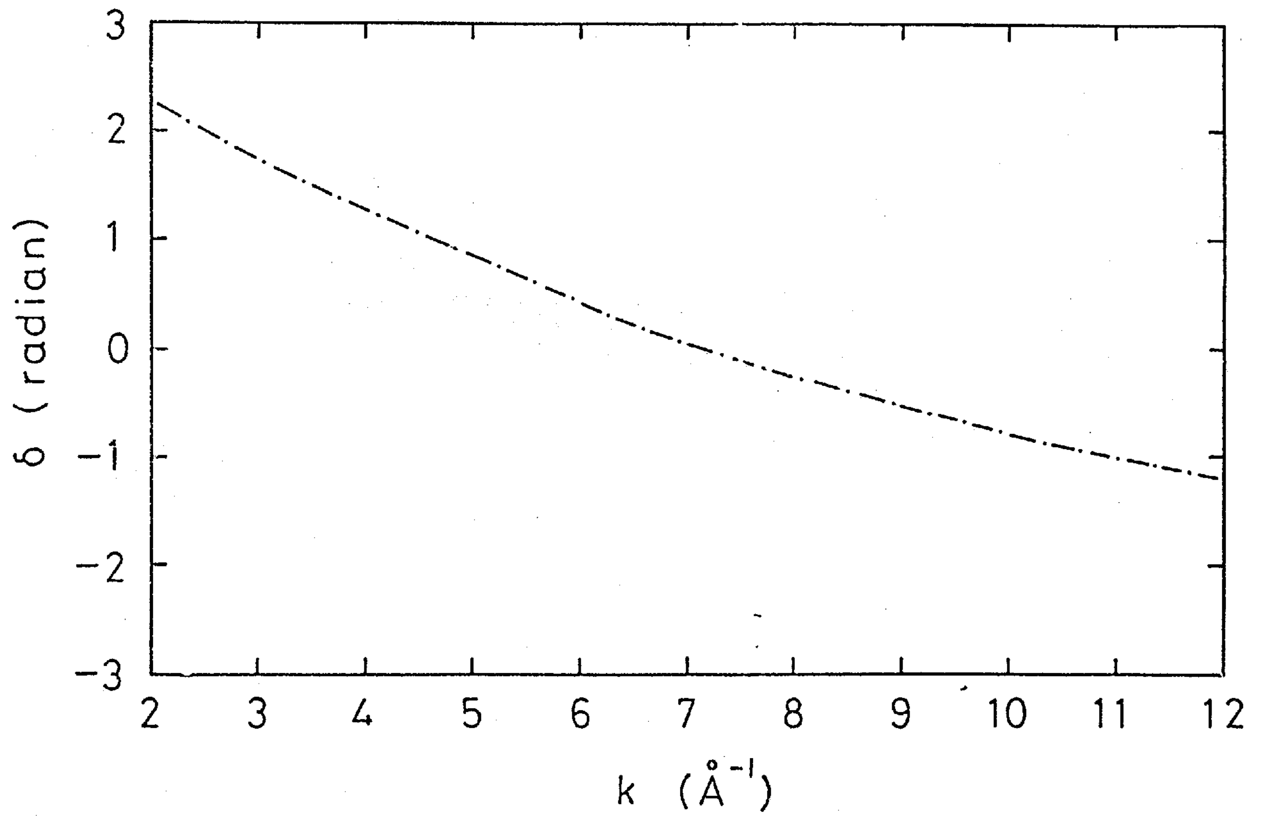

Fig.2 Central atom phase shift by germanium atom as a function of photoelectron wave number k, calculated using Herman and Skillman wave functions.

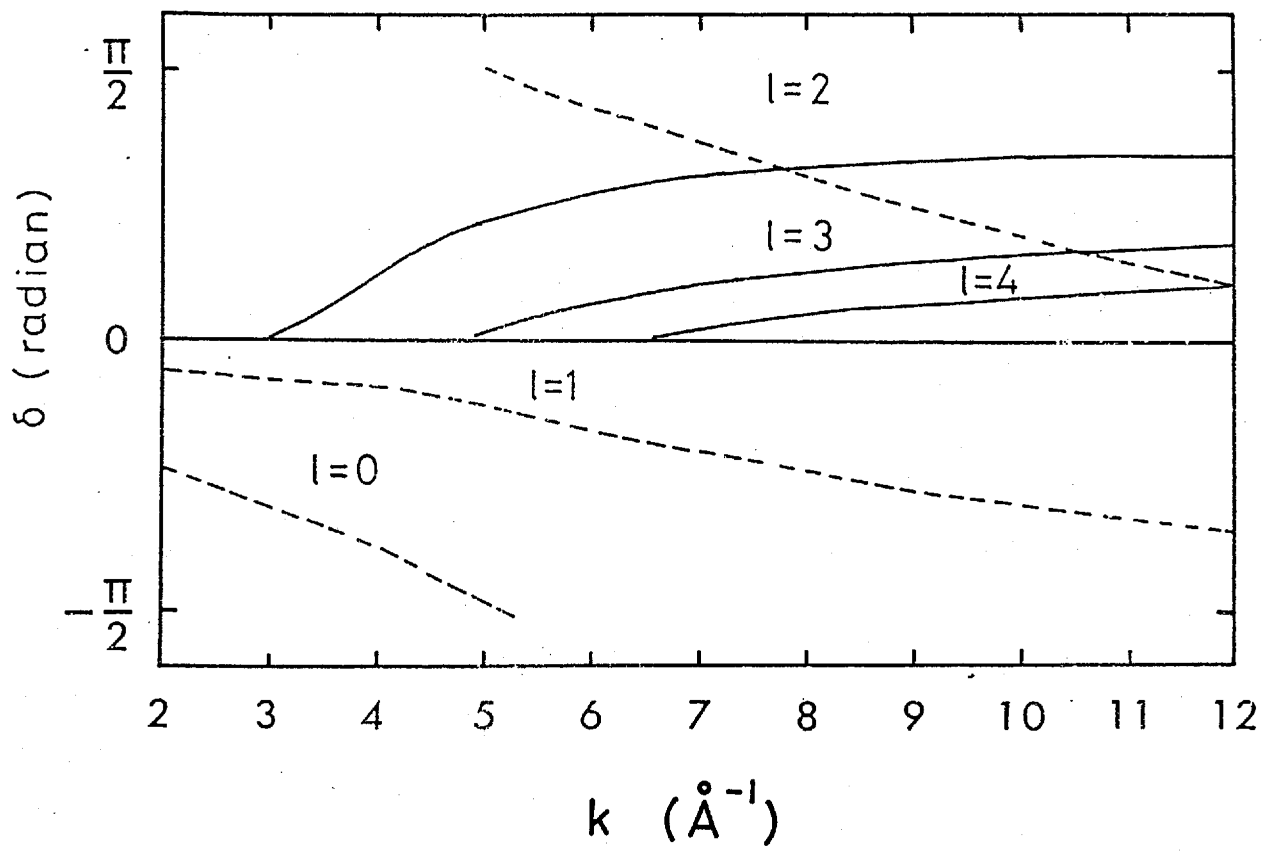

Fig.3 Phase shift of electron scattering by silicon atom for l=0, 1, 2, 3, 4 as a function of photoelectron wave number k.

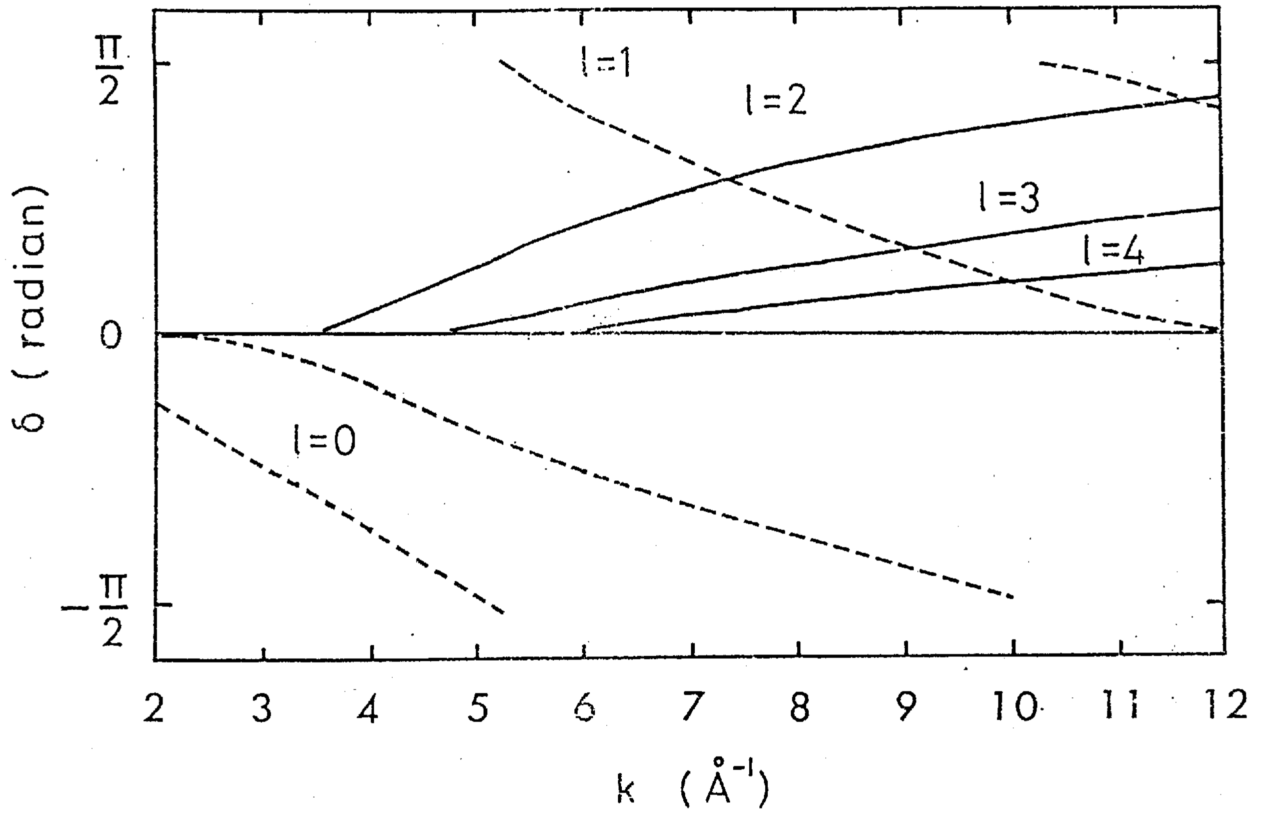

Fig.4 Phase shift of electron scattering by germanium atom for l=0, 1, 2, 3, 4 as a function of photoelectron wave number k.

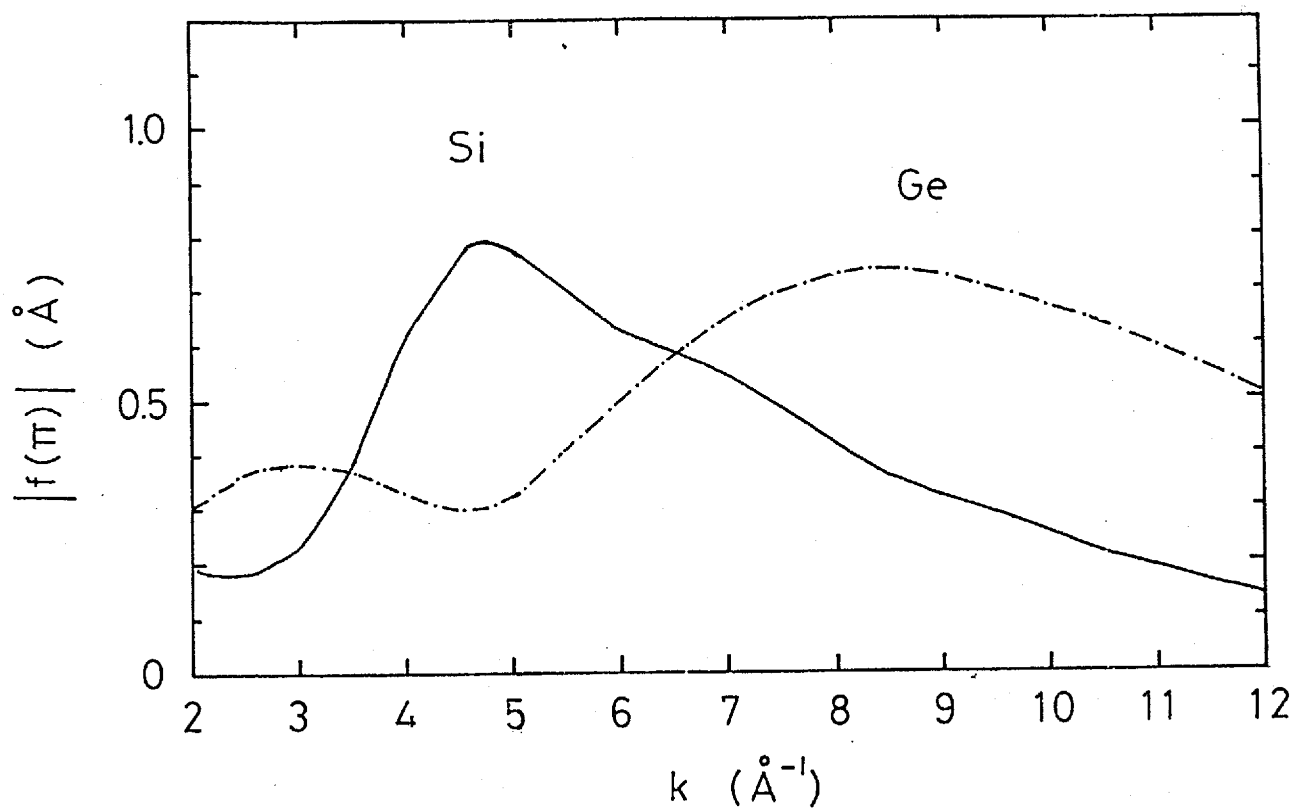

Fig.5 The absolute value of backscattering amplitude of silicon (solid line) and germanium (dashed-dotted line) atoms as a function of photoelectron wave number k. Thermal Debye parameters, $\overline{B_{293}}$, are taken to be zero in both cases.

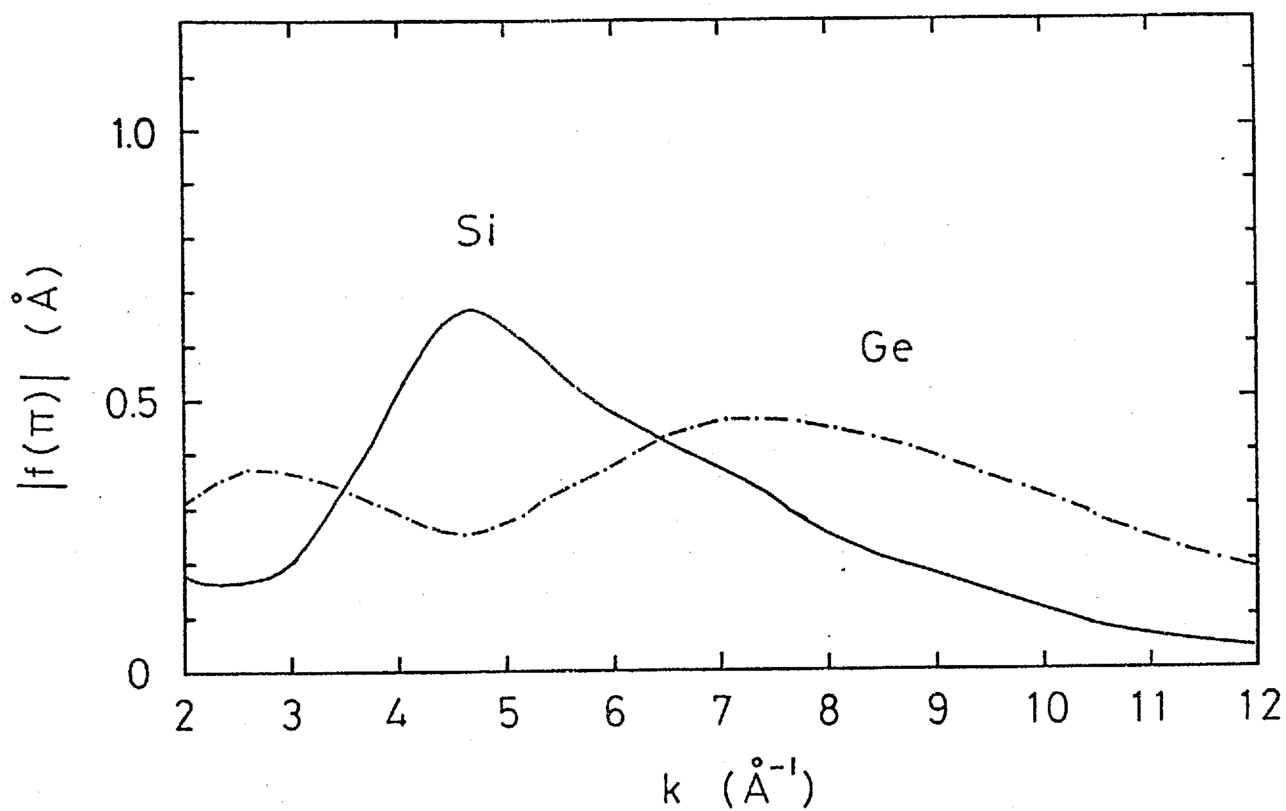

Fig.6 The absolute value of backscattering amplitude of silicon (solid line) and germanium (dash-dotted line) atoms as a function of photoelectron wave number k. Thermal Debye parameters, $\overline{B_{293}}$, are taken to be 0.31 and 0.30, respectively, for silicon atom and germanium atom.

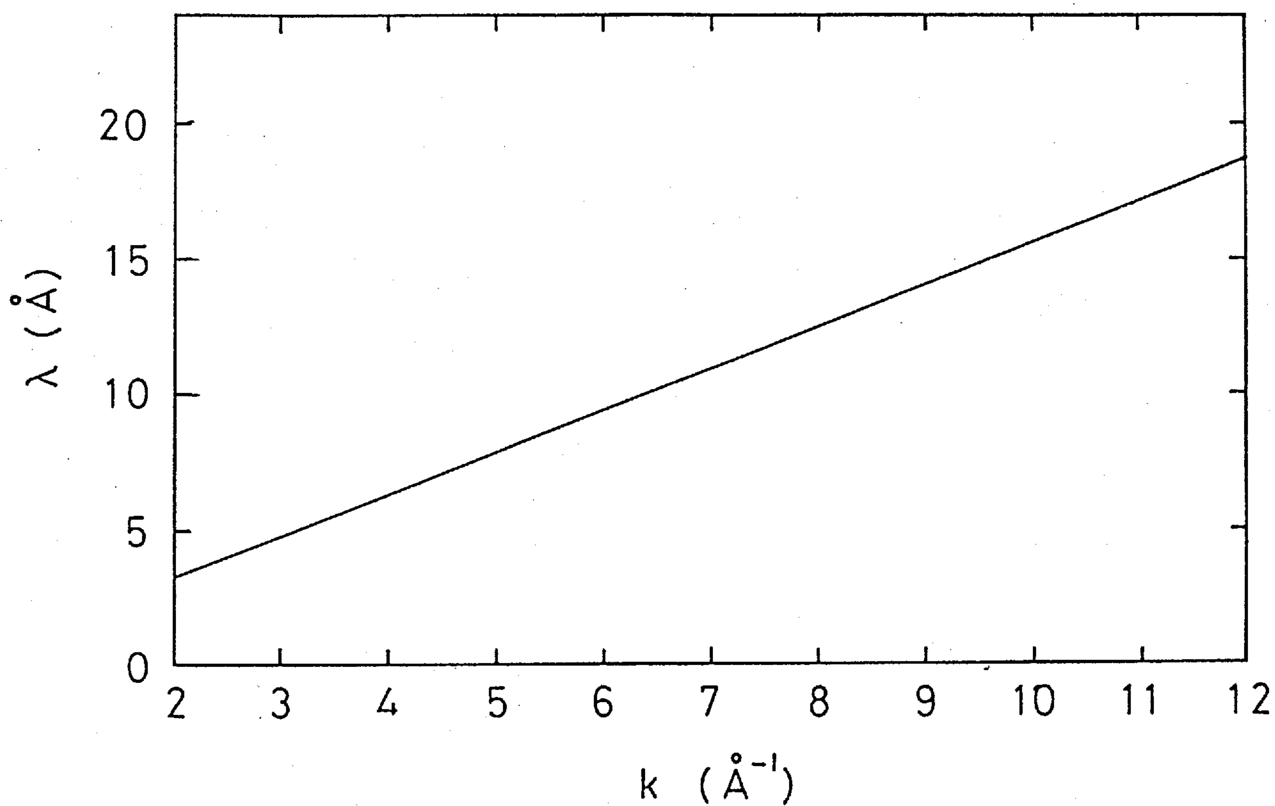

Fig.7 Escape depth of crystalline germanium as a function of photoelectron wave number k.

3.2 Plane wave analysis

The curve-fitting method with the EXAFS formula (5)[3,16] based on the plane wave expression of emitted photoelectrons, has been tried to analyze experimental EXAFS for a-$Si_{1-x}Ge_x$:H. In calculations, bond lengths and Debye-Waller factors for Ge-Ge and Ge-Si, coordination numbers of Ge and Si atoms around Ge atoms, and absorption edge energy, E_0, for the Ge-Ge bond and the Ge-Si bond were employed for fitting parameters.

Figure 8 shows the deviation of E_0 values for Ge-Ge and Ge-Si bonds from its steepest points at the absorption edge-jump. Apparently E_0 values for the Ge-Ge and Ge-Si bonds differ from each other and they deviate from the origin by maximum of 20 eV. However, the threshold of photoelectron-emission should be almost the same no matter how electronic configurations of X-ray absorbing atoms differ with different bonds.

Figure 9 shows bond lengths for the Ge-Ge and Ge-Si bonds. Determined bond lengths and their dependence on composition appears to be plausible. However, it should be emphasized here that it is hard to accept resulting bond lengths because E_0 values differ from each other, to a physically unreasonable extent through the curve- fitting procedure, as shown in Fig. 8.

The absorption edge energy, E_0, is the most fundamental quantity in EXAFS analysis since it defines the wave number of emitted photoelectrons. The curve-fitting method is a way to obtain the results regardless of physical meanings of parameters. Thus, it is necessary to interpret the determined values carefully, even if the calculated oscillation is in good

agreement with the experiment.

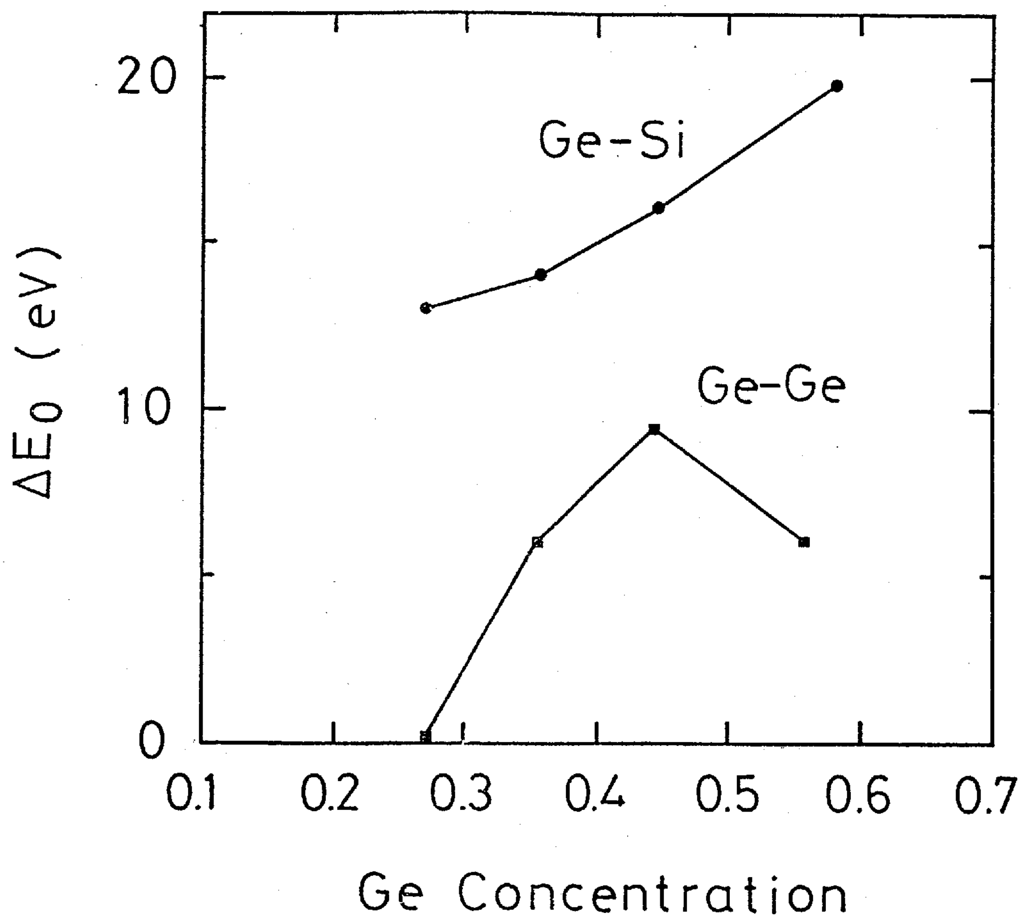

Fig.8 Deviation of the absorption edge energy, E_0, from the steepest point at the edge-jump optimized for the Ge-Ge bond and the Ge-Si bond.

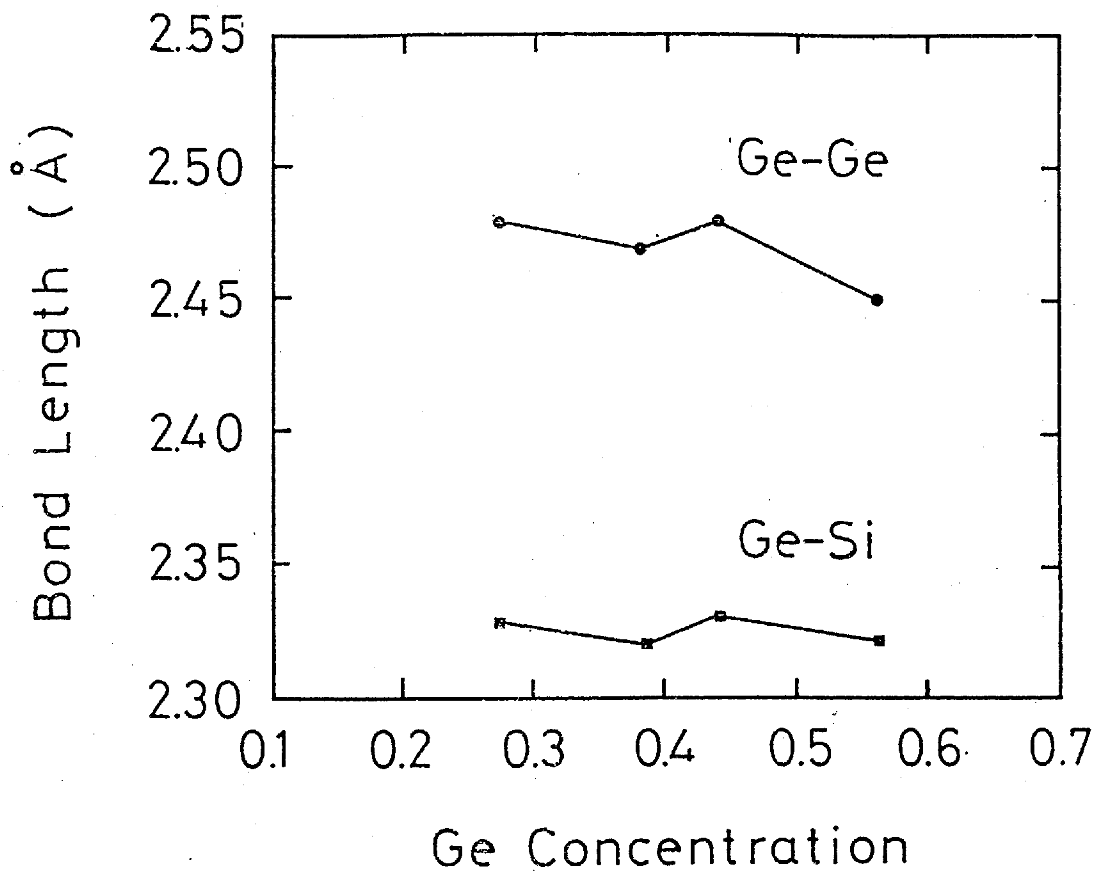

Fig.9 Bond lengths for the Ge-Ge bond and the Ge-Si bond obtained by the curve-fit analysis based on the plane waves of emitted photoelectrons.

3.3 Spherical wave analysis

The experimental Ge K- edge EXAFS for a-$Si_{0.62}$ $Ge_{0.38}$:H is shown by the solid line(a) in Fig. 10. The photoelectron wave number as the abscissa is converted from the X-ray energy via an absorption edge energy of 11.109keV defined as the steepest point in the experimental absorption curve. The $\chi(k)$ was multiplied by k^3 to intensify the amplitude at higher k values. Good fitting with a theoretical curve was realized at the Ge coordination ratio, 0.4, and the bond lengths, 2.46Å for Ge-Ge cand 2.41Å for Ge-Si as shown by the dashed-dotted line (b) in the figure. As for the phase and period of the EXAFS, the solid line (a) is in good agreement with the dashed-dotted line (b) over a range of k from 4.5 to 12 $Å^{-1}$.

The Ge-K edge EXAFS for a-$Si_{1-x}Ge_x$:H has been analyzed by Minomura et al.[24] and Incoccia et al.[25] However, their results , although generally excellent, contain some ambiguities because of the lack of model compounds.

Incoccia et al.[25] have used the conventional formula[3,16] and extracted the backscattering amplitude and the phase shift for the Ge-Ge and Ge-Si bonds from experiments on a-Ge:H and a-$Si_{0.93}Ge_{0.07}$:H. The E_0 value in that work was taken at the inflection point at the edge-jump. It was concluded that the Ge-Ge bond length and the Ge-Si bond length were 2.45Å and 2.37Å, respectively, for x = 0.37 - 0.72.

The Ge-Ge bond lengths in Incoccia's and the present author's results were very close. However, the Ge-Si bond lengths differed by 0.04Å. The EXAFS calculated by using

Eq.(3) with Incoccia's results are shown by the dotted line (c) in Fig. 10. The Ge coordination ratio was assumed to be 0.4. The dotted line is considerably different from the solid one for a whole range of the wave number k. The E_0 value alone cannot account for this discrepancy. Thus, it is unfortunately difficult to explain the present experiment with the results in Ref. 25.

The theoretical EXAFS for two extreme cases are shown in Fig. 11. One is the EXAFS when the absorbing Ge atom is surrounded only by Ge atoms (solid line (a)). The other case is obtained when it is surrounded only by Si atoms (dotted line (b)). The Ge-Ge bond length and the Ge-Si bond length were set to be 2.46Å and 2.41Å, respectively. The phase difference for these two cases increases at the lower k value. Because the phase and period of EXAFS oscillation is sensitive to a slight change of coordinating atom, we can determine the coordination ratio with high accuracy in the a-$Si_{1-x}Ge_x$:H case.

The calculated EXAFS oscillations are shown in Fig. 12, where the Ge coordination ratio is 0.3 (dotted line (a)), 0.4 (solid line (b)) and 0.5 (dashed -dotted line (c)). The Ge-Ge bond length and the Ge-Si bond length were set to be 2.46Å and 2.41Å, respectively. It is clearly easy to distinguish one spectrum from another. Thus, the accuracy of the coordination ratio is within 0.05.

As for the amplitude of the EXAFS, it is hard to say that a good agreement is obtained. The amplitude is affected by the thermal vibration of atoms and the inelastic scattering of photoelectrons. In the present analysis, Debye parameters,

$\overline{B_{293}}$, for crystals at room temperature were employed. Strictly speaking, the $\overline{B_{293}}$ values for crystals are different from amorphous materials. Incoccia et al. have also discussed Debye-Waller factors, σ^2, for the Ge-Ge bond and the Ge-Si bond. It was concluded in the paper that the σ^2 for both bonds have almost the same value and do not change with Ge concentration. Accordingly, in the case of a-Si_{1-x} Ge_x:H, the $\overline{B_{293}}$ value for crystals were used unless it is necessary to determine the absolute coordination number, N_{Ge} or N_{Si}. Additionally, the effect of the inelastic scattering of photoelectrons should be the same for the Ge-Ge bond and the Ge-Si bond. It must be emphasized that the fine adjustment of the phase and period of EXAFS oscillation as employed in the present analysis can provide accurate local structure except for the absolute coordination number.

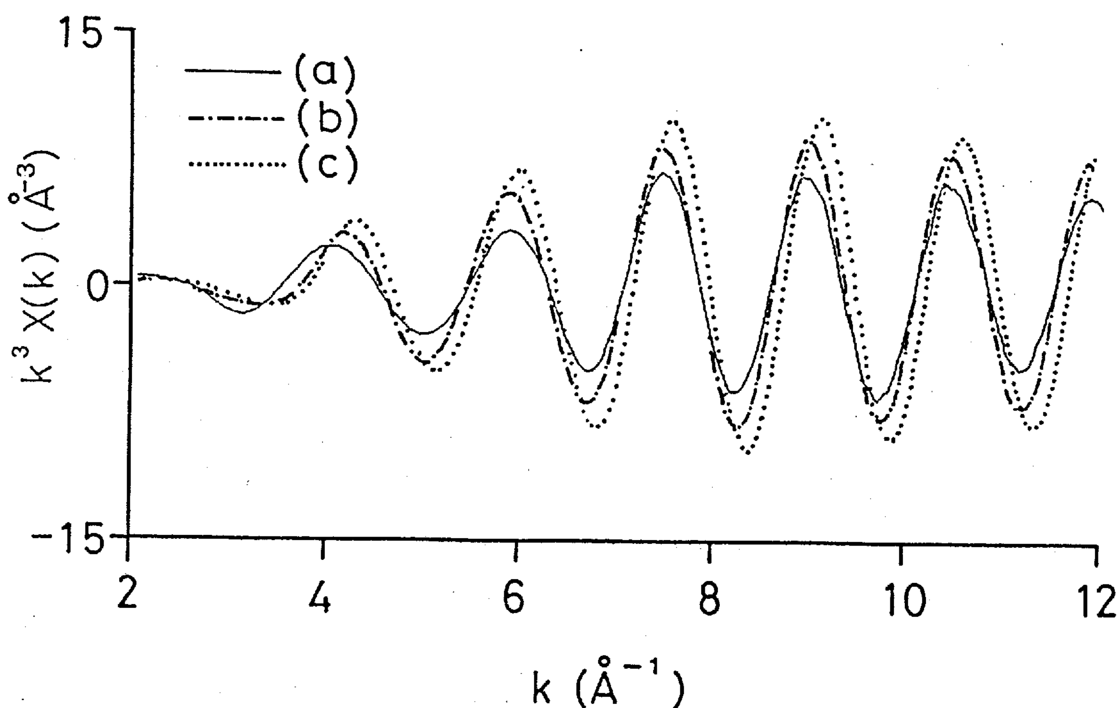

Fig.10 Comparison of theoretical and experimental EXAFS for a-$Si_{0.62}Ge_{0.38}$:H. The total of coordination number around Ge atom is assumed to be 4 in (b) and (c).

(a) Experimental Ge-K EXAFS.
The energy of absorption edge E_0 is taken at the steepest point in the edge-jump.

(b) Theoretical EXAFS calculated using Eq.(3) for the Ge coordination ratio, 0.4 and the bond lengths, 2.46Å for Ge-Ge and 2.41Å for Ge-Si.

(c) Theoretical EXAFS calculated using Eq.(3) for the Ge coordination ratio, 0.4 and the bond lengths, 2.45Å for Ge-Ge and 2.37Å for Ge-Si.

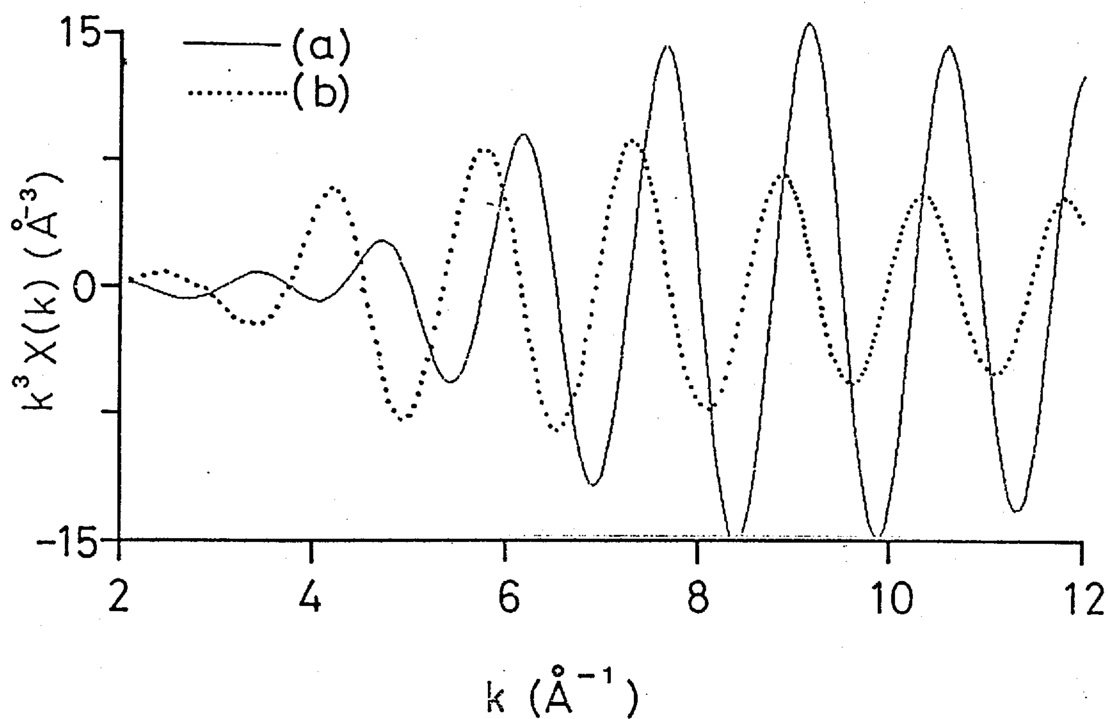

Fig.11 Theoretical EXAFS for two extreme cases: (a) Ge atom is surrounded by Ge atoms only (solid line) and (b) Ge atom is surrounded by Si atoms only(dashed-line). The total of coordination number around Ge atom is assumed to be 4.

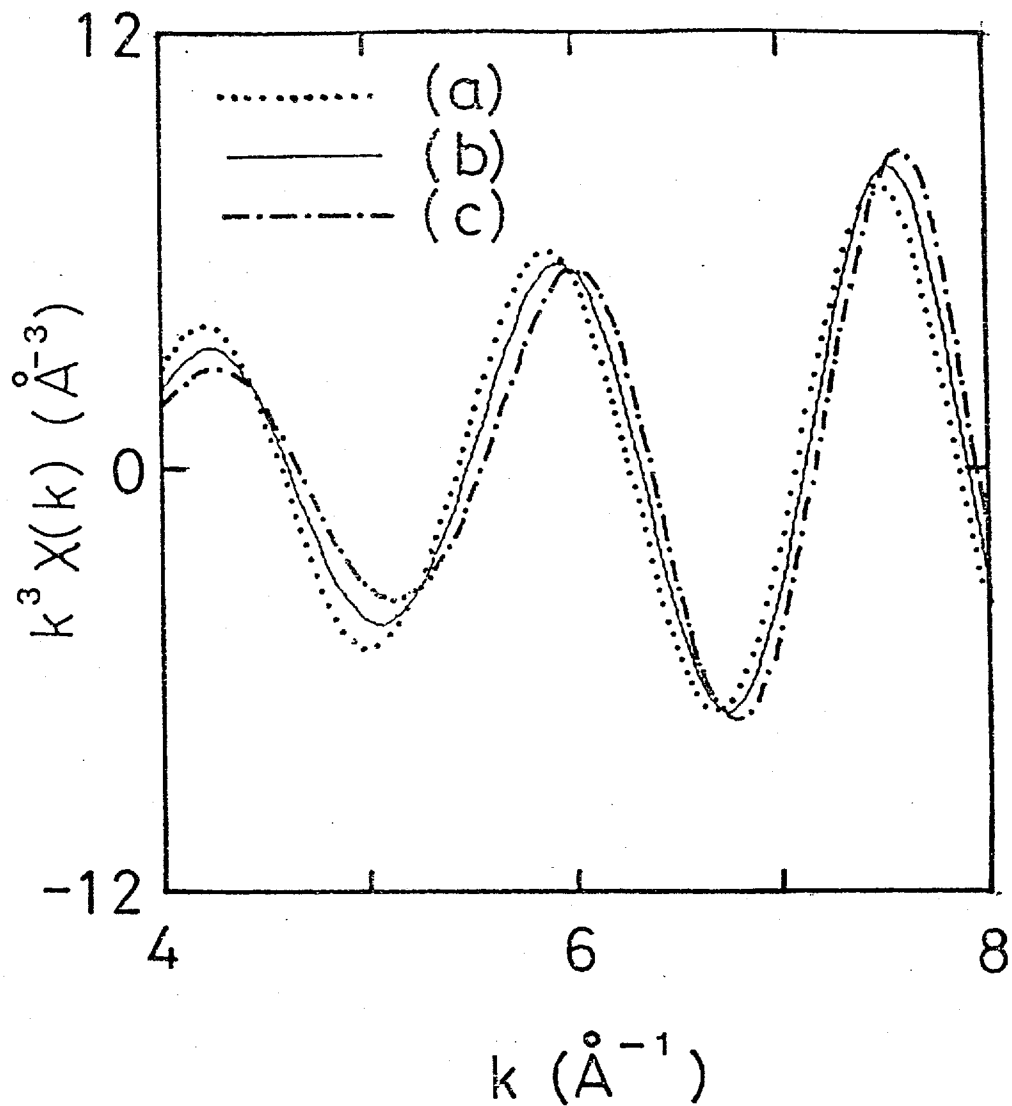

Fig.12 Change in EXAFS with Ge coordination ratio of (a) 0.3 (dotted line), (b) 0.4 (solid line) and (c) 0.5 (dashed-dotted line).

3.4 Absorption edge energy problem

It has been pointed out that the optimum E_0 in the conventional analysis with or without using model compounds has different value for each bond[6]. In this section, we demonstrate how EXAFS oscillation derived from the conventional formula Eq.(5) are different from those from the spherical wave approach and then discuss how optimum E_0 values for Ge-Ge and Ge-Si bonds differ from the absorption edge energy, when we determine them through curve-fitting technique by using Eq. (5).

The EXAFS oscillation due to the Ge-Ge bond calculated by using a strict expression Eq.(3) is represented by the solid line (a) in Fig.13. The dotted line (b) shows the result obtained through the use of the conventional equation (5). The Ge-Ge bond length was 2.46Å in both cases. The EXAFS oscillation for the dotted line is quite different from that for the solid line, especially at a low energy. The phase difference in both cases is about 12eV and 3eV at a photoelectron energy of 100eV and 500eV, respectively.

The EXAFS oscillation due to the Ge-Si bond calculated by using a strict expression (3) is represented by the solid line (a) in Fig. 14. The dotted line (b) shows the same calculated by using the asymptotic equation (5). The Ge-Si bond length was set to 2.41Å. The phase difference for these two cases is about 5eV and 3eV at a photoelectron energy of 100eV and 500eV, respectively.

It should be noted that the phase difference in Fig.13 and Fig. 14 is not constant and increases as the photoelectron

energy becomes smaller. It is because the second term of the asymptotic expansion in Eq. (4), $l(l+1)/2\rho$, depends on the photoelectron energy and the interatomic distance. The term, $l(l+1)/2\rho$, cannot be neglected for photoelectron energy up to 500eV when the Ge-Ge bond length is 2.46Å and the Ge-Si bond length is 2.41Å. Asymptotic Eq. (5) is only valid for a more distant electron path. For example, in the case of the fourth nearest Cu-Cu bond of Cu metal, whose interatomic distance is 5.11Å, Eq. (5) almost agrees with Eq.(3) down to 100eV of the photoelectron energy.[15]

The absorption coefficient near the Ge K-edge for a-$Si_{0.62}Ge_{0.38}$:H is shown in Fig. 15. The arrow A shows the E_0 value employed in the present analysis. Arrows B and C show the optimum E_0 in Eq. (5) for Ge -Ge and Ge-Si bonds at the photoelectron energy of 100 eV, respectively. Clearly, the arrows B and C are out of the edge region. Maximum discrepancy of optimum E_0 for the Ge-Ge and the Ge-Si bonds are about 7eV at a photoelectron energy of 100eV. Although it has not been confirmed that the point of the steepest change corresponds to the absorption edge, only one fixed energy is allowed to be the absorption energy. In the curve-fitting analysis with the Eq.(5), the best fit is achieved with the different value for each bond: maximum discrepancy is 22.27eV for the Mo-S and Mo-Fe bonds.[6] However, as pointed out above, the optimum E_0 cannot be uniquely defined over a wide range of photoelectron energy as far as only the Ge-Si bond is concerned. So real information about the structure cannot be obtained with Eq. (5) no matter how the E_0 value for each bond is optimized.

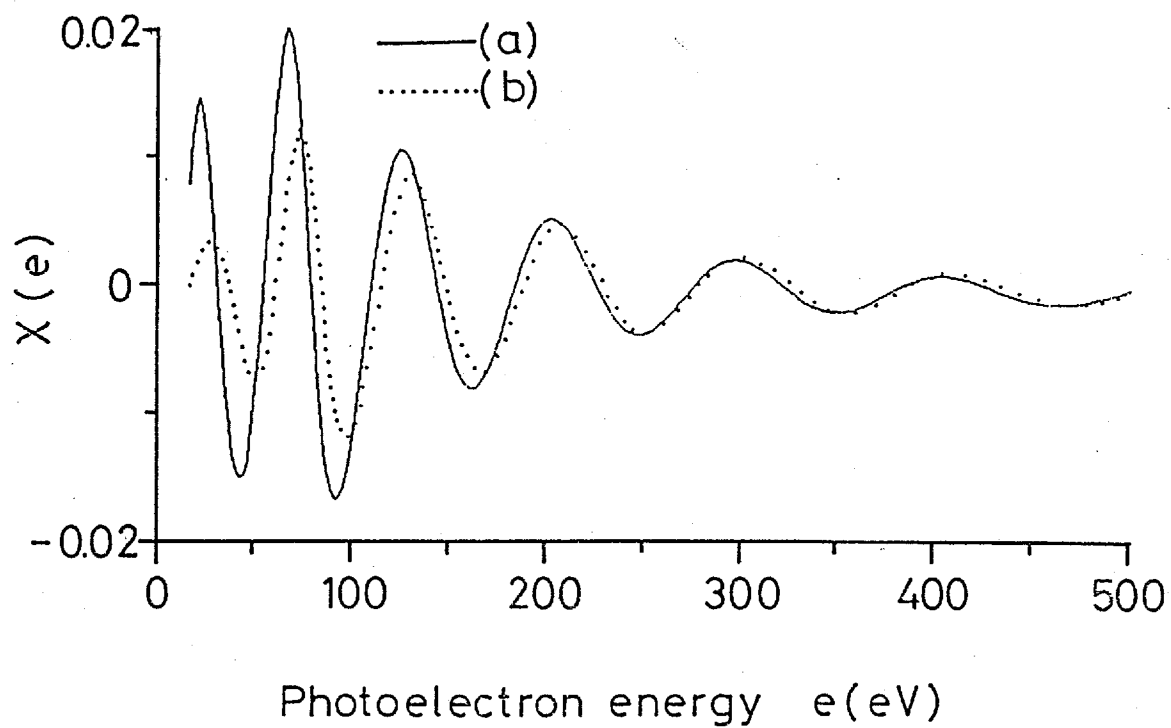

Fig.13 Comparison of theoretical EXAFS for Ge-Ge bond whose bond length is 2.46Å.

(a) calculated using Eq.(3)

(b) calculated using Eq.(5)

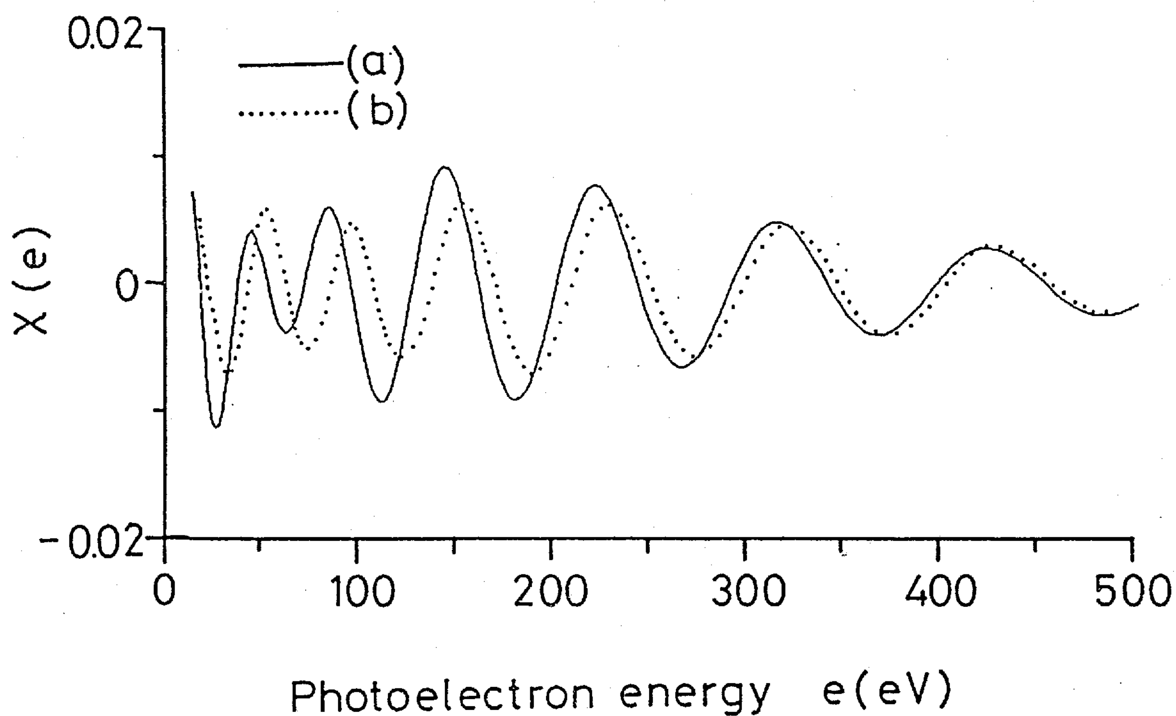

Fig.14 Comparison of theoretical EXAFS for Ge-Si bond whose bond length is 2.41Å.

(a) calculated using Eq.(3)

(b) calculated using Eq.(5)

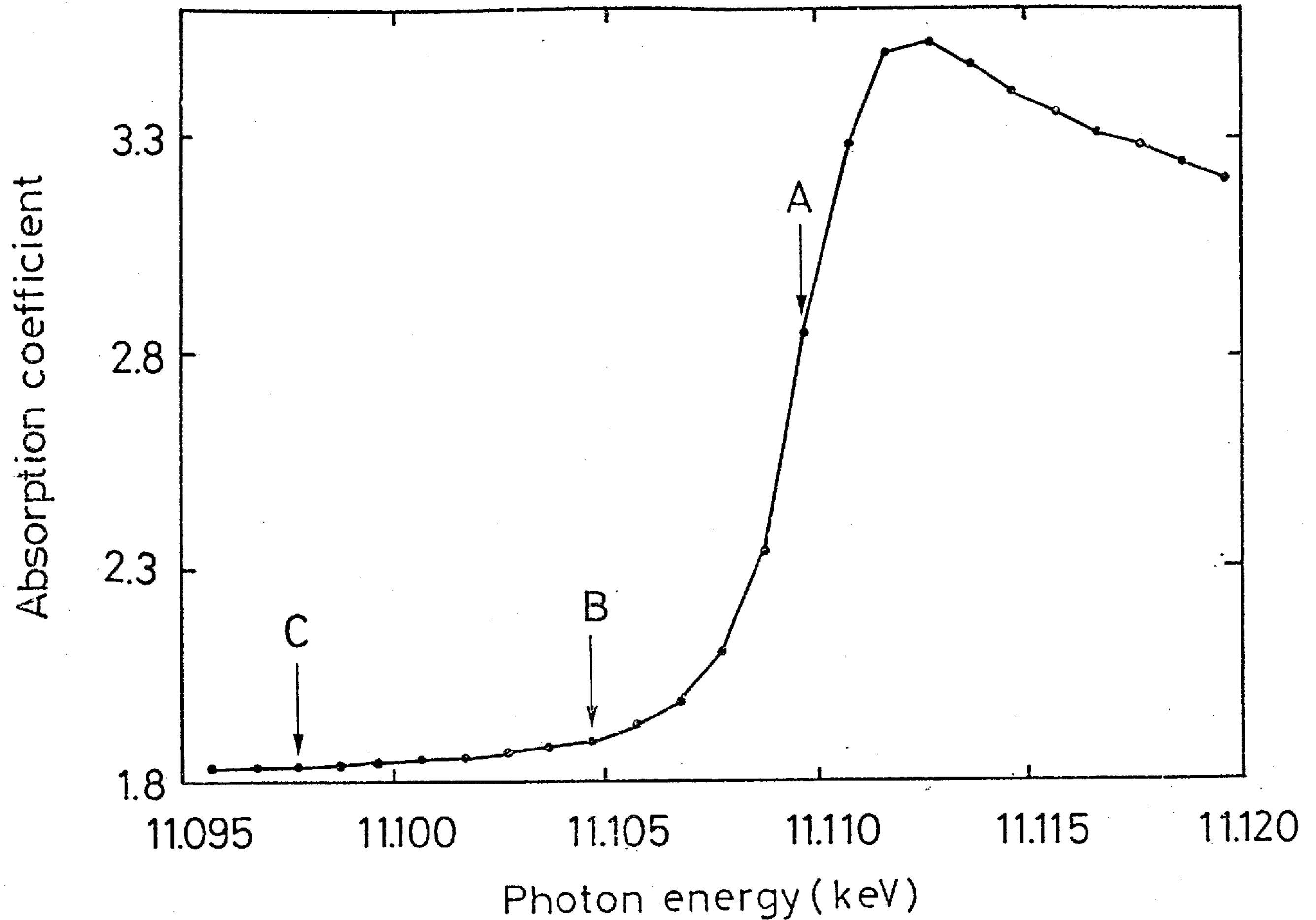

Fig.15 The absorption coefficient near the Ge K- edge for a-$Si_{0.62}Ge_{0.38}$:H. The absorption edge energy E_0 in the present analysis is pointed by the arrow A. The arrows B and C point the optimum E_0 values in Eq.(5) for Ge-Si and Ge-Ge bonds at a photoelectrons energy of 100 eV, respectively.

4. DISCUSSION

4.1 Amorphous Silicon-Germanium alloys (a-$Si_{1-x}Ge_x$:H)

Hydrogenated amorphous silicon-germanium alloys(a-$Si_{1-x}Ge_x$:H) have been attracting much attention in the development of high-efficiency photovoltaic solar cells.[26,27] It is well known that the optical band gap can be narrowed by increasing the Ge concentration in the alloys. However, the photoelectric properties[28] deteriorate with increasing Ge concentration. Recently, it has been suggested that structural inhomogeneity in the alloys may be responsible for the interior photoelectric properties. One might expect that a strong correlation exists between the electrical and structural properties. In order to shed light on these problems, close examination of the local structure is essential. Given that these films are amorphous, the use of the extended X-ray absorption fine structure (EXAFS) technique[2] is the most promising way to determine the structure.

In the above section, a fine adjustment technique, which is based on the spherical wave expression of photoelectrons, was presented. The new technique was first employed to analyze the Ge K-edge EXAFS for a-$Si_{0.62}Ge_{0.38}$:H. It is known that a-$Si_{1-x}Ge_x$:H forms a family of materials for which model compounds (that is, crystalline alloys with the same composition and well-known structure) are difficult to obtain over the whole compositional range. Using the fine-adjustment technique, which does not require the use of model compounds, good agreement has been

obtained between the experimental data and calculated ones without correcting the absorption-edge energy.

In the present study, EXAFS spectra above the Ge K-edge in a series of a-$Si_{1-x}Ge_x$:H alloys with various Ge concentration have been measured. Figure 16 shows the normalized Ge K-edge EXAFS oscillations for a-$Si_{1-x}Ge_x$:H; (a) x=0.27, (b) x=0.38, (c) x=0.56, (d) x=1.0. These are plotted as a function of the photoelectron wave number, k, and the normalized EXAFS , $\chi(k)$, is multiplied by k^3. It is clearly seen that the amplitude of the EXAFS oscillation around k=8 $Å^{-1}$ increases with increasing Ge concentration. This variation in the EXAFS oscillation could be caused by a difference in backscattering amplitude of the atoms which form the coordination around Ge atom as shown in Fig. 5 and Fig. 6; the backscattering amplitude function for the Ge atoms has a peak near k=8 $Å^{-1}$. The above result indicates that the coordination of Ge atoms surrounding Ge atoms increases with incresing Ge concentration in the films.

These EXAFS spectra were analyzed according to the procedures described in the section 3.3 to determine the Ge-Ge and the Ge-Si bond lengths and the coordination ratio of Ge atoms.

Figure 17 shows the Ge-Ge bond length, R_{Ge-Ge}, and the Ge-Si bond length, R_{Ge-Si}, in a-$Si_{1-x}Ge_x$:H films as a function of the Ge concentration x. In the figure, the bond lengths in Ge crystals (c-Ge) and Si crystals (c-Si) are indicated by the arrows. The error bars result from the fitting procedure in which the bond lengths were varied by 0.005 Å. It is clear that both the Ge-Ge and the Ge-Si bond lengths are constant throughout

the entire compositional range. This composition-independent bond length seems to be a general feature of disordered alloys.[25,29] In the present analysis, the Ge-Ge bond length agrees well with that in the Ge crystals (2.45Å), while the Ge-Si bond length is close to the average value of the bond lengths for both Ge and Si crystals.

As mentioned before, Incoccia et al.[25] analyzed Ge K-edge EXAFS for a-$Si_{1-x}Ge_x$:H, employing a conventional curve-fitting technique and derived values of 2.45Å and 2.37-2.38 Å for the Ge-Ge bond and the Ge-Si bond lengths, respectively. Although the Ge-Ge bond lengths obtained in both studies are very close to each other, the Ge-Si bond lengths obtained in Ref.25 is 0.03-0.04 Å smaller than that in the present study. This discrepancy in the Ge-Si bond length is far beyond the experimental ambiguity. This difference in bond lengths can be attributed to the way of EXAFS analysis.[3,16] The examination in the section 3.4 clarified that the best-fitting result in conventional curve-fitting can be possibly obtained when the absorption-edge energy is corrected for Ge-Ge and Ge-Si bonds, using results from model compounds. In the EXAFS study in Ref. 25, the value of the edge energy assumed to be equal to the energy position of the main inflection point of the Ge K-edge. However, it is impossible to correct the edge energy adequately for Ge-Si bonds since there are no appropriate model compounds for all a-$Si_{1-x}Ge_x$:H alloy are not available. These problems could have led to the underestimation of the Ge-Si bond length.

In contrast to this, the present calculated spectra are in

good agreement with the experimental ones throughout the entire compositional range without a correction of edge energy. Considering that the bond length in amorphous Si is 2.35-2.37 Å,[30] we can conclude that the Ge-Si bond length in a-$Si_{1-x}Ge_x$:H films is exactly equal to the mean value of the bond length in amorphous Ge and that in amorphous Si.

Figure 18 shows the coordination ratio of Ge atoms surrounding a central Ge atom as a function of the Ge concentration x. Note that the Ge concentration is a mean composition which is a typical macroscopic property of the alloys, while the Ge coordination ratio, $N_{Ge}/(N_{Ge} + N_{Si})$, gives to the local composition of Ge atoms surrounding a central Ge atom. The error bars result from the fitting procedure in which the coordination ratios of the Ge and Si atoms were varied by 0.05, respectively. In Fig.18 , if Ge and Si atoms were randomly mixed over the whole compositional range in the alloys, one would expect the Ge coordination ratio to increase linearly with the Ge concentration as shown by the dotted line. Such being the case for $x<0.4$, it follows that Ge and Si atoms are randomly mixed in this Ge concentration range. With increasing Ge concentration, however, the Ge coordination ratio is found to be 15-20 percent higher than that expected for a random mixture of both atoms. The last result stands in contrast with the former EXAFS experiments of a-$Si_{1-x}Ge_x$:H[24,25] which demonstrated random mixing over the whole compositional range. Nevertheless, the deviation of the Ge coordination ratio for Ge-rich alloys is considered to be significant in the present analysis.

In order to illustrate the significance of the deviation in the Ge coordination ratio, an example of the fitting results for the Ge K-edge EXAFS for a-$Si_{0.44}Ge_{0.56}$:H is shown in Fig. 19. In the computations, the Ge-Ge and Ge-Si bond lengths were assumed to be equal to 2.46Å and 2.41 Å, respectively, while the coordination ratios of Ge and Si atoms were varied by 0.05. It should be noted here that the phase and period in theoretical EXAFS oscillations in the k range from 4 to 8 $Å^{-1}$ is sensitively dependent on the coordination ratio of each atom. This is because the Ge-Ge and Ge-Si pairs contribute to EXAFS oscillations differently in both phase and period at small k. First, the experimental EXAFS curve(a) (solid-line) was compared with the theoretical curve(b) (dotted line) which was computed assuming the Ge coordination ratio of 0.55. Although the Ge coodination ratio is close to that expected for a Ge concentration of 0.56, the agreement between the experimental and the theoretical EXAFS curve is satisfactory for neither phase nor period. In addition, it should be stressed that the theoretical curve (b) could by no means be fitted to the experimental curve (a) even by correcting the absorption edge energy. The experimental EXAFS curve (a) is found to be in better agreement with the theoretical curve (c) (dashed line) which was computed assuming a Ge coordination ratio of 0.65. One may point out the disagreement in the amplitude of EXAFS oscillation between the theoretical and the experimental curve. The magnitude of the amplitude is affected by the thermal vibration of atoms and inelastic scattering of photoelectrons. The theoretical and

experimental EXAFS curves can be fitted better by adjusting the Debye parameter and the mean free path of photoelectrons. It should be emphasized, however, that in the present study, artificial modification of these parameters are not needed in order to determine the coordination ratio. In the same manner as described above, the best-fit result for the Ge K-edge EXAFS for a-$Si_{0.53}Ge_{0.47}$:H was obtained when the Ge coordination ratio was equal to 0.57.

The above results show that the Ge coordination ratios in Ge-rich films are 15-20 percent higher than those expected on the basis of the Ge concentrations. This means that the Ge-rich films employed in the present study are structurally somewhat inhomogeneous. The origin of this inhomogeneity could be explained qualitatively in several ways by considering various microstructures in Ge-rich films. If Si atoms in the films had a tendency to form segments of polysilane chains[31] $(SiH_2)_n$ with increasing Ge concentration, the Ge coordination ratio would be increased. Such segments can be detected by infrared(IR) absorption measurement. However, IR measurements in this study did not support the above assumption; i.e., the fraction of polysilane chains remained almost unchanged, independent of the Ge concentration. Another possibility is that a heterostructure is formed which is composed of small cluster-like Ge-rich regions on a microscopic scale. Our transmission electron microscope observation did not reveal any discernible microstructure in the Ge-rich films, in contrast to the observations by Mackenzie et al. [28] It seems reasonable to assume the structural inhomogeneity in the distribution of Ge atoms, although separated phase of high

Ge-rich density are not found.

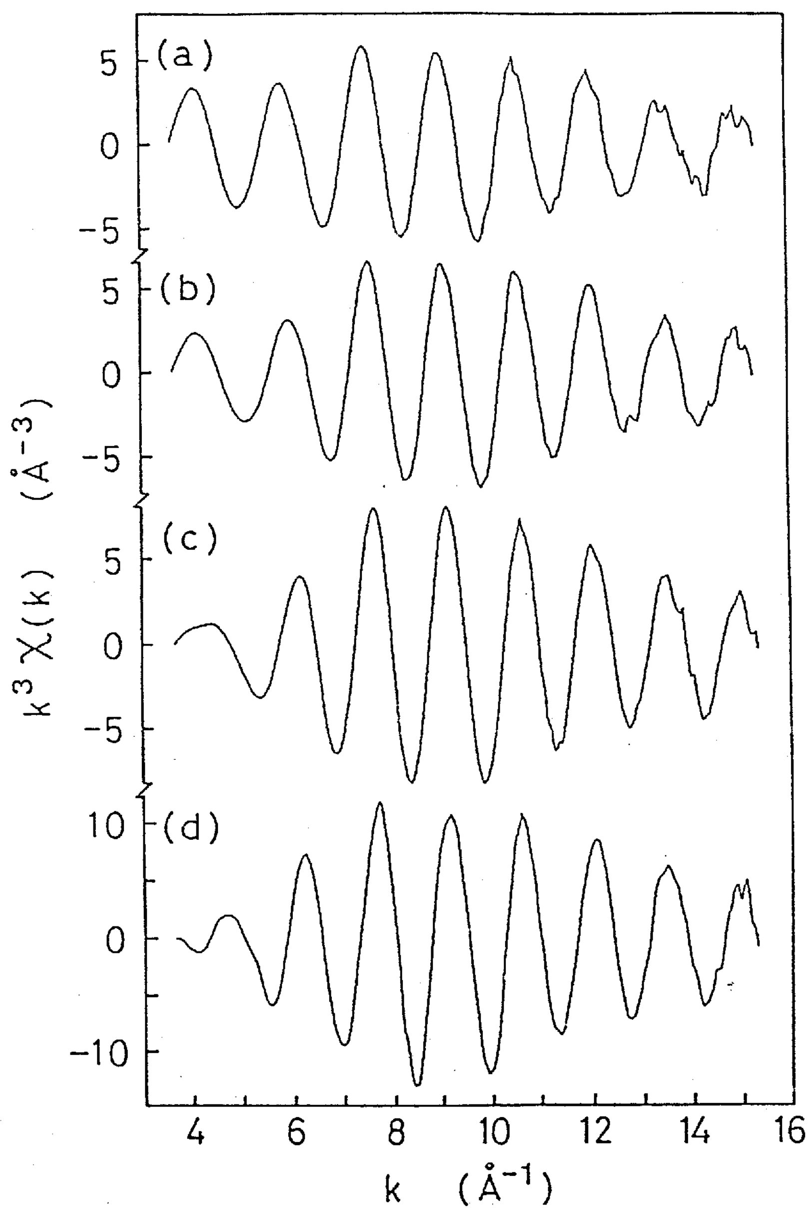

Fig.16 Ge K-edge EXAFS oscillations for a-$Si_{1-x}Ge_x$:H at different Ge concentrations x; (a)x=0.27, (b)x=0.38, (c)x=0.56, (d)x=1.0, plotted as a function of the photoelectron wave number k.

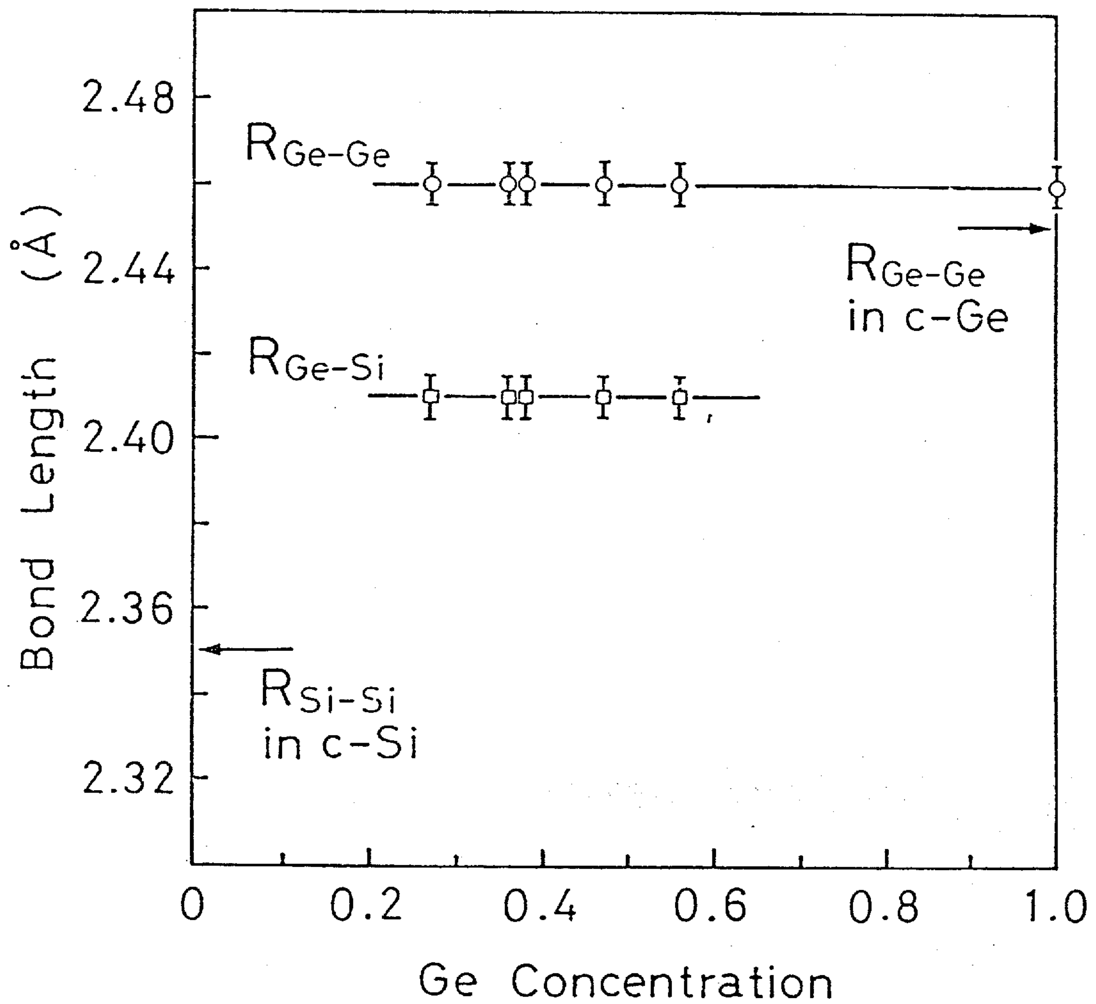

Fig.17 Ge-Ge bond length R_{Ge-Ge} (open circles) and Ge-Si bond length R_{Ge-Si} (open squares) as a function of Ge concentration x in a-$Si_{1-x}Ge_x$:H. The bond lengths are concentration independent and equal to R_{Ge-Ge}=2.46Å and R_{Ge-Si}=2.41 Å, respectively. The bond lengths in Ge crystals (c-Ge) and Si crystals (c-Si) are indicated by arrows.

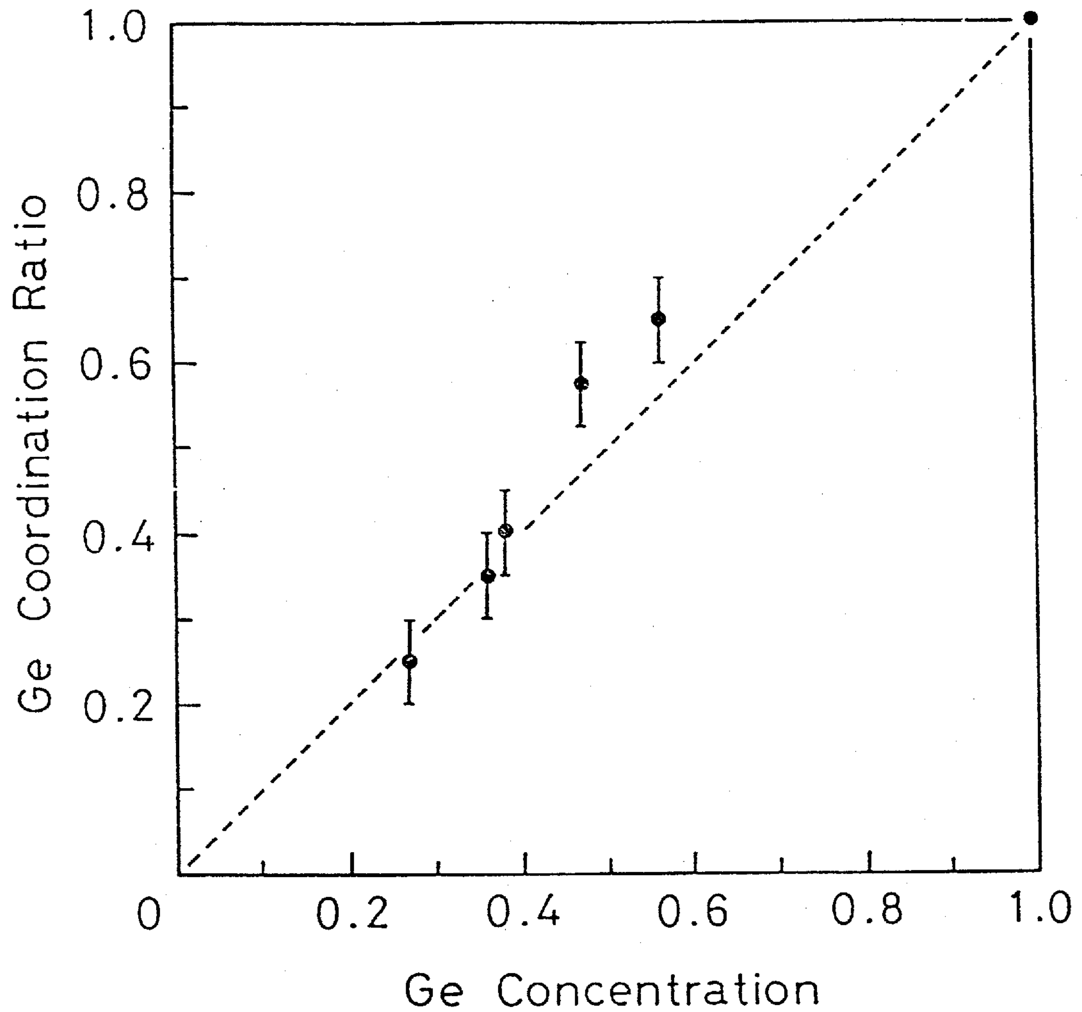

Fig.18 Ge coordination ratio around Ge atoms, $N_{Ge}/(N_{Ge} + N_{Si})$, as a function of Ge concentration x in a-$Si_{1-x}Ge_x$:H. The dashed line shows the Ge coordination ratio expected for a random mixture of Si and Ge atoms.

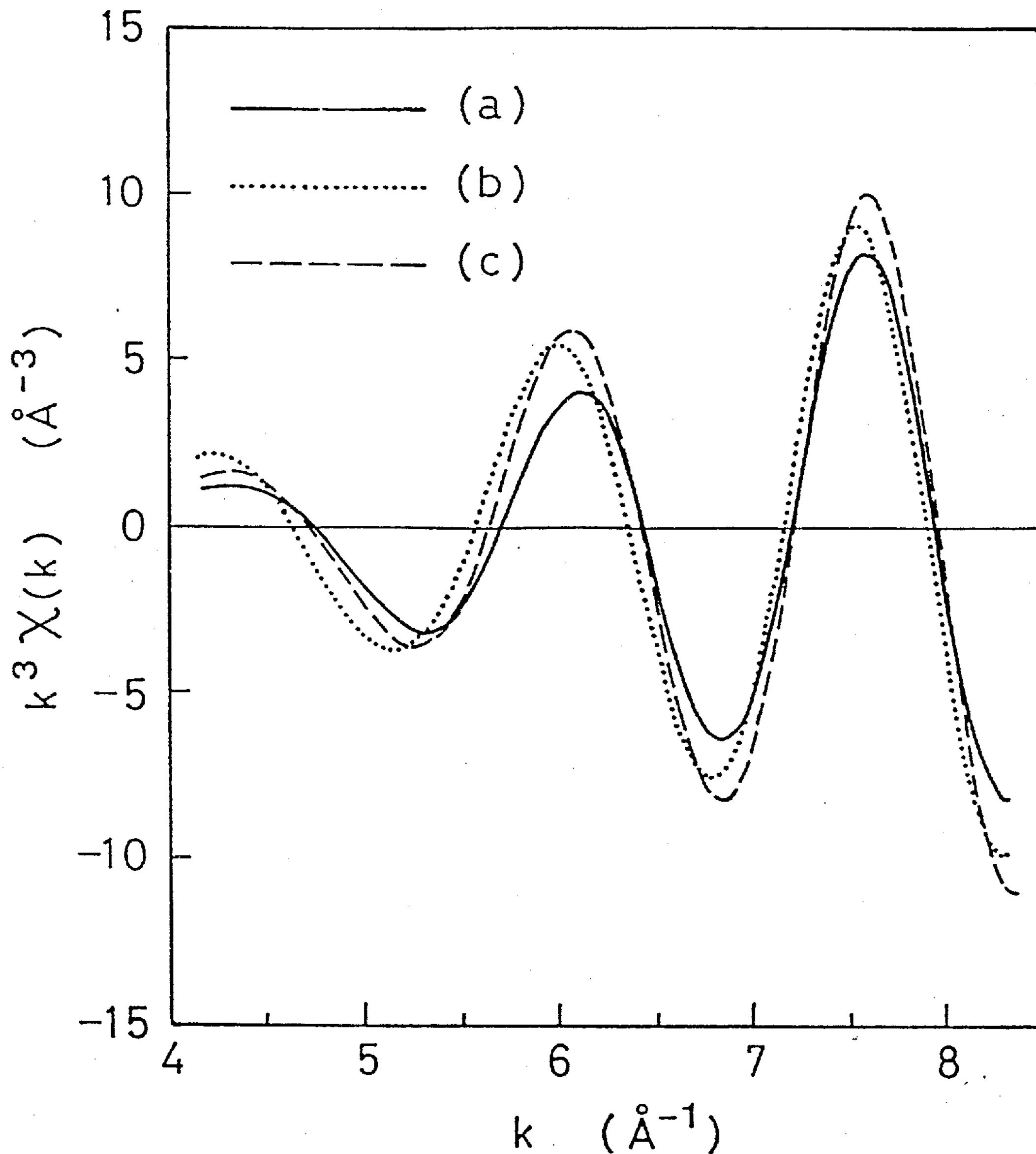

Fig.19 Comparison of experimental Ge K-edge EXAFS oscillation for a-$Si_{0.44}Ge_{0.56}$:H (a) (solid line) with theoretical EXAFS oscillations (b), (c); curve (b) (dotted line) was calculated for a Ge concentration ratio($N_{Ge}/(N_{Ge}+N_{Si})$) of 0.55 and curve (c) (dashed line) for 0.65. In the calculations, the Ge-Ge and the Ge-Si bond lengths were assumed to be 2.46Å and 2.41Å, respectively.

4.2 Crystalline Silicon-Germanium alloys (c-$Si_{1-x}Ge_x$)

Crystalline silicon- germanium alloys attract much attention both from fundamental and industrial points of view because of their valuable properties, i.e. continuous change of lattice constant[32,33] and band gap[33] associated with concentration. Despite that the alloys are known to form liquid-solutions over an entire compositional range, its local structures such as bond length and coordination, etc., still remain almost unknown.

How atoms form crystal with a specific structure is an essential question. Recently atomic structures on microscopic scale in alloys have been studied intensively in regard to thermodynamic properties.[34,35] Crystal structure in alloys is characterized by the lattice constant determined by X-ray diffraction measurement. However, since lattice constant is an average over a unit cell in alloys, it does not provide us with further information on nearest-neighbor atoms. Huang[36] has suggested, from the X-ray diffuse scattering measurement, that some distorted lattice structures exist in alloys, despite that alloys conserve structure system similar to their host materials. However, studies focused on distorted structures in the alloys have not been accumulated so much, because there is not straightforward way to determine distorted structures from diffuse scattering.

EXAFS is a promising probe to study microscopic structure around the atoms of specific elements in alloys. By the EXAFS measurements of c-$Si_{1-x}Ge_x$ with several kinds of Ge concentration, the bond lengths for Ge-Ge and Ge-Si and

coordinations of the nearest sites for Ge and Si atoms were evaluated.

Figure 20 shows the EXAFS oscillations, $\chi(k)$, versus photoelectron wave number, k, due to the nearest-neighbor atoms around a Ge atom, which were extracted through the Fourier filtering technique. The experimental EXAFS spectra were analyzed by a curve-fit technique with the formula based on the spherical wave expression of emitted photoelectrons.

Figure 21 shows the dependence of determined Ge coordination ratio on the composition. If atoms are distributed homogeneously, Ge coordination ratio is identical to Ge concentration. EXAFS analysis shows that the Ge coordination ratio is almost equal to the Ge concentration, as shown in Fig. 21, which means homogeneous distribution in $Si_{1-x}Ge_x$ alloys with composition ranging from 0.19 to 0.81.

Figure 22 shows the dependence of bond length for Ge-Ge and Ge-Si on composition. It is interesting that bond length does not vary with composition, and that bond lengths are distinctly different for each bond: 2.45Å for Ge-Ge and 2.40Å for Ge-Si.

Two opposite concepts for bond length dependence on composition in alloys were presented. First, Bragg[37] and then Pauling[38] noted that bond lengths in alloys are the sum of atomic radii, hence should be composition independent (Bragg's limit). Second, Vegard[42] discovered that lattice constant, a(x), changes linearly with thecomposition, x;$a(x)=(1-x)a_1+xa_2$, where a_1 and a_2 are lattice constants at the end-point materials, x=0 and x=1, respectively. Thus bond length is considered to vary according to lattice constant. For example,

in a diamond structure, bond length is given simply as $\sqrt{3}\,a(x)/4$ (Vegard's limit).

Martins and Zunger[34] have investigated the lattice distortions around isovalent impurities using a valence force field theory.[40,41] They defined the dimensionless relaxation parameter in ternary ($A_{1-x}B_xC$) alloys as

$$\varepsilon = (R_{BC}(AC{:}B)-R_{AC})/(R_{BC}-R_{AC}), \tag{6}$$

where R_{AC} and R_{BC} are bond lengths at pure and end-point material, respectively, and $R_{BC}(AC{:}B)$ is the BC bond length around the B impurities in the AC host crystal. They predicted that ε is closer to Bragg's limit (ε=1) than Vegard's limit (ε=0); ε =0.6-0.8 for most semiconductors.

On the other hand, Ito[35] has estimated value for III-V ternary semiconductor alloys using a pseudopotential perturbation theory. The calculated results of ε are in the range of 0.2 to 0.3 for most $A_{1-x}B_xC$ alloys. Therefore the bond lengths are closer to the Vegard's limit (ε=0) than to the Bragg's limit(ε=1).

On the contrary to the theoretical calculations, EXAFS results on ternary semiconductor alloys seem to support the Bragg and Pauling notion. EXAFS study of $Ga_{1-x}In_xAs$ alloys [42] shows that the Ga-As and In-As nearest neighbor distances remain nearly constant, varying only by 0.04A; ε=0.82 for $Ga_{1-x}In_xAs$. In $GaAs_{1-x}P_x$ systems,[43] the Ga-As and Ga-P nearest-neighbor disbtances also differ from each other, showing slight variations with composition; ε=0.60 for $GaAs_{1-x}P_x$.

In the present study for binary alloys, however, it has been shown that bond lengths in crystalline $Si_{1-x}Ge_x$ alloys are constant over composition x from 0.2 to 0.8, hence then bonds relax completely in the IV-IV alloys; 2.45Å for Ge-Ge bond and 2.40Å for Ge-Si bond. They are almost identical to the sum of their atomic radii, wehere the atomic radii of 1.22 Å for Ge and 1.17Å for Si. Although bond lengths for Si-Si in alloys have not been investigated in the present study, it is expected to be the same in crystalline Si in the analogy of Ge-Ge and Ge-Si bonds because Si atoms are covalently bonded. Accordingly, our result also supports the Bragg and Pauling notion.

It should be noted that results on ternary systems were obtained using a curve-fit analysis with a conventional single-scattering formula for EXAFS, which was based on plane waves of emmitted photoelectrons. In conventional analysis, it is extremely difficult to have reliable estimation of bond lengths in alloys, although possible corrections on phase shifts functions due to backscattering give satisfactory results. Therefore their results, although excellent, have to be reconsidered prudently for the quantitative discussion. It is difficult to discuss whether small variation of bond lengths with composition is characteristic in ternary alloys or not. In either case, it is satisfactory to consider that bonding elements determine bond lengths in semiconductor alloys as Bragg and Pauling noted.

Bond angle modification is essential to form a unit cell with a bond of a distinct length. By Pauli's exclusion principle, strong repulsive interaction acts between covalently

bonded atoms. Considering that a diamond structure is comparatively empty, it is more advantageous to conserve bond lengths. Therefore structural change would rather occur in bond angles than bond lengths.

As shown in Fig. 21, atoms are randomly mixed in the alloys. Accordingly, in triangle configurations of Si-<u>Ge</u>-Si, Ge-<u>Ge</u>-Ge, and Ge-<u>Ge</u>-Si (underlines represent central atoms), bond angles must be also distinctly fixed for each configuration. Thus, if bond angle distributions could be measured, the shape of distribution profile might be dependent on the Ge concentration. Figure 23 shows lattice constant dependence on composition in the alloys. Lattice constant varies with composition, and slight deviation from Vegard's law is recognized. It should be noted that deviation increases in the medium compositional range. One can expect that the degree of bond angle distortion would approaches its maximum value at mid-point composition, provided that bond lengths between randomly mixed atoms are invariant with composition. Accordingly, a nonlinear variation in a lattice constant as shown in Fig. 23 would be a consequence of invariant bond lengths.

In the previous section, local structures of a-$Si_{1-x}Ge_x$:H alloys have been studied. It was concluded that bond lengths for Ge-Ge and Ge-Si are 2.46Å and 2.41Å, respectively, and that atoms are randomly mixed below the Ge concentration of 0.40. Bond lengths for Ge-Ge and Ge-Si are almost the same in amorphous and crystalline alloys. Accordingly it can be concluded that bond angle distribution is a primary factor, in the IV-IV alloys,

to distinguish crystalline alloys from amorphous alloys.

Bond lengths that are the sum of atomic radii are found in covalent and ionic materials.[42] On the other hand, it is interesting to examine whether the Bragg and Pauling notion hold also for metallic alloys. Two groups performed EXAFS study on Cu-Al alloy and reported the contradicting results: 2.72 Å[44] and 2.79Å.[45] The nearest-neighbor distances in Cu and Al are 2.55Å and 2.86Å, respectively. If interatomic distances are determined by the sum of atomic radii as Pauling noted, it should be 2.70Å. It seems to be a worthwhile subject to determine metallic bond distances in order to examine the essential properties of atomic bonds.

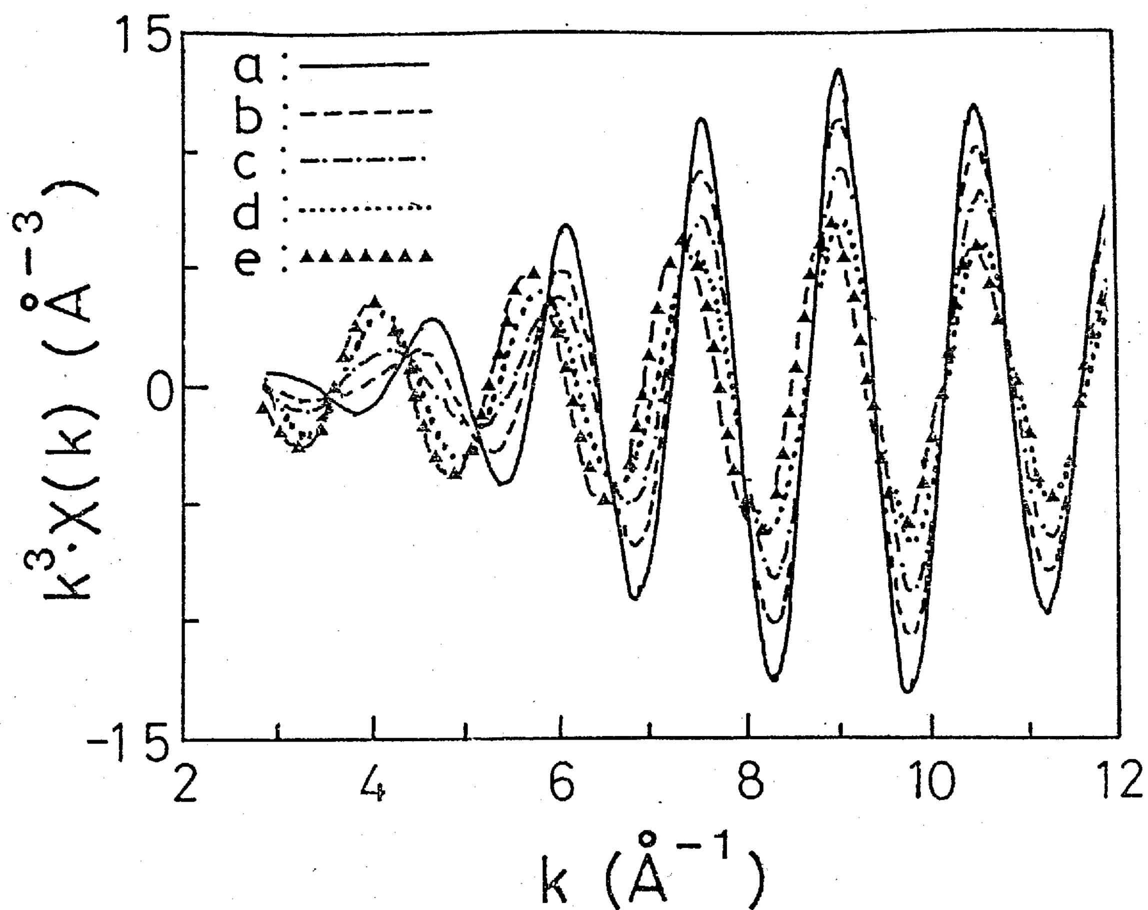

Fig.20 Normalized Ge K-edge EXAFS oscillation for crystalline $Si_{1-x}Ge_x$ alloys at different Ge concentrations x; (a)=1.0, (b)= 0.8, (c)= 0.6, (d)=0.4, (e)=0.2, plotted as a function of wave number k.

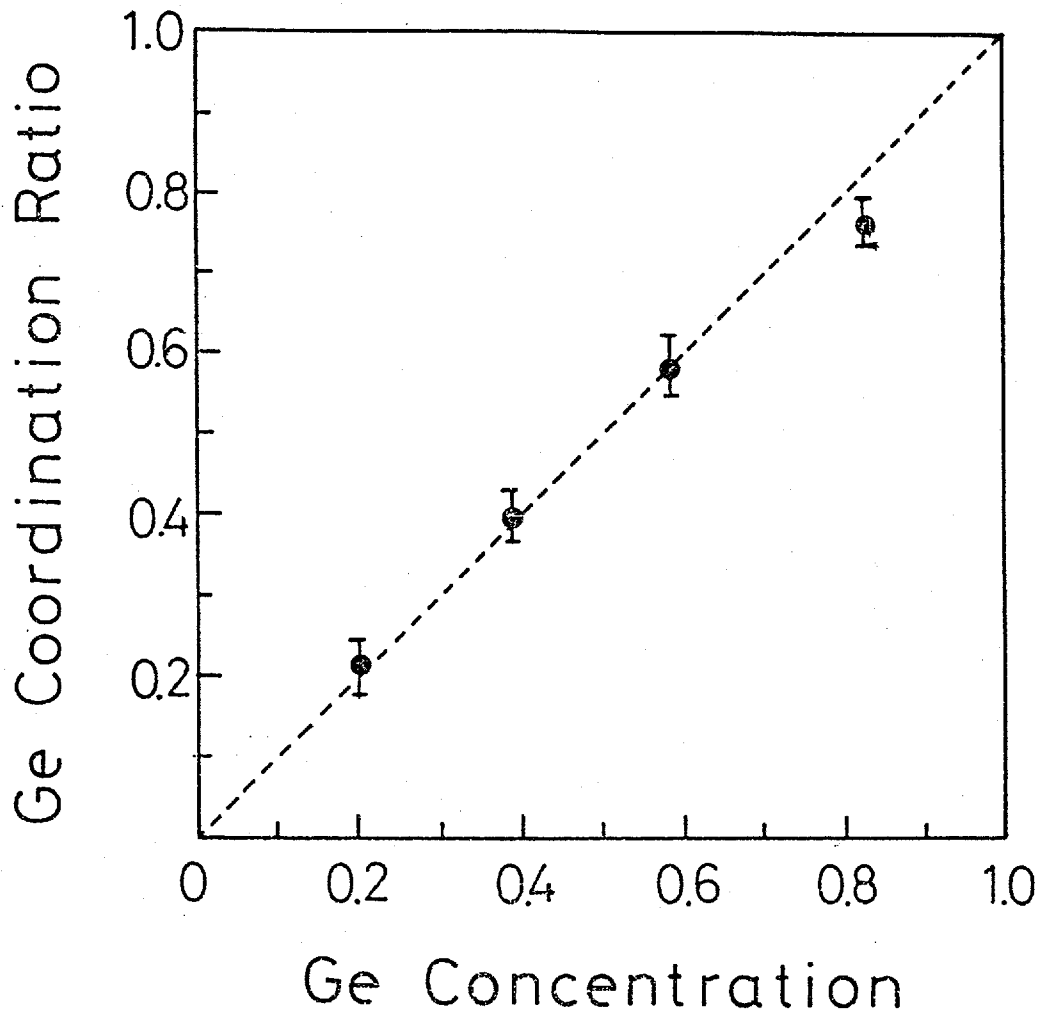

Fig.21 Ge coordination ratio around Ge atoms, $N_{Ge}/(N_{Ge}+N_{Si})$, as a function of Ge concentration x in crystalline $Si_{1-x}Ge_x$ alloys. The dashed line shows the Ge coordination ratio expected for a random mixture of Si and Ge atoms.

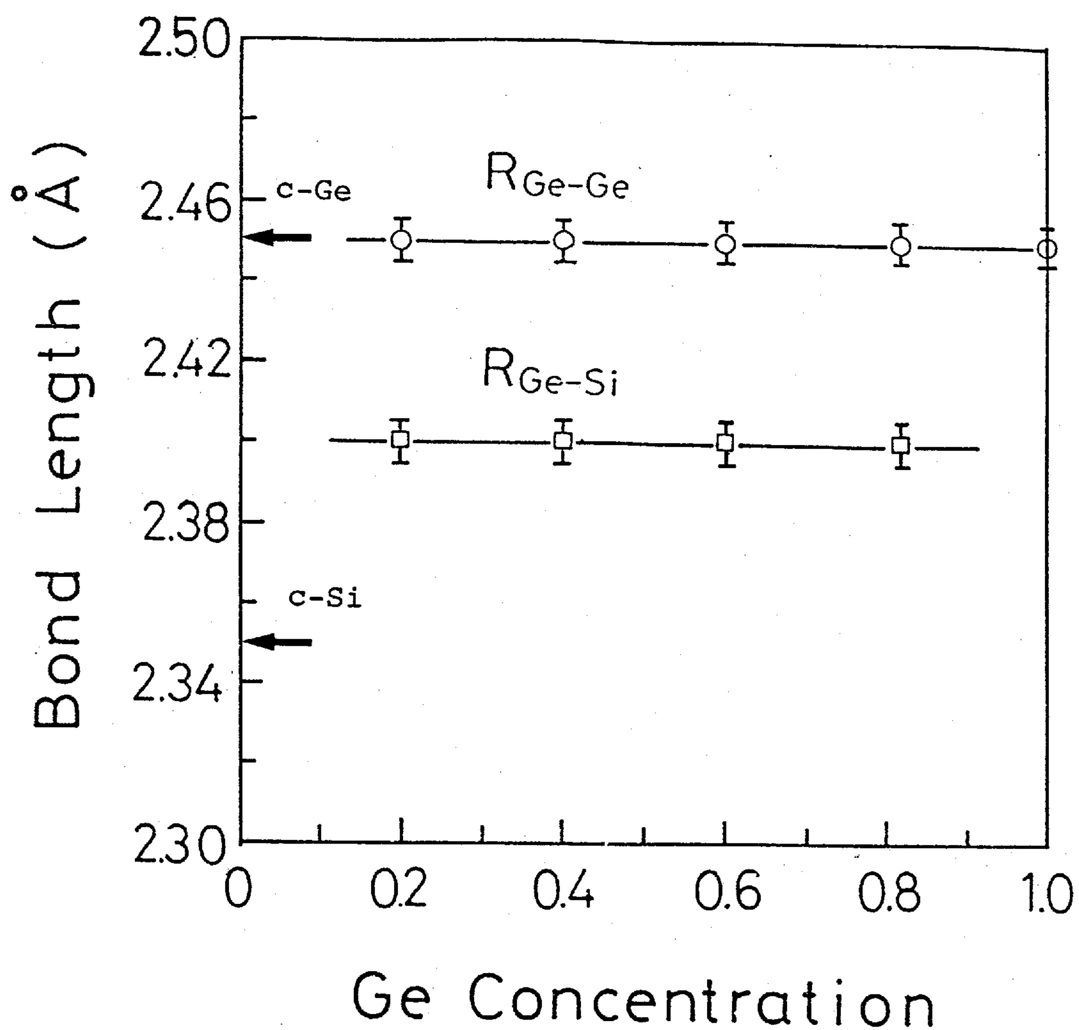

Fig.22 Ge-Ge bond length R_{Ge-Ge} (open circles) and Ge-Si bond length R_{Ge-Si} (open squares) as a function of Ge concentration in crystalline $Si_{1-x}Ge_x$ alloys. The bond lengths are concentration independent and equal to R_{Ge-Ge}= 2.45 Å and R_{Ge-Si}=2.40 Å, respectively. The bond lengths in Ge crystals (c-Ge) and Si crystal(c-Si) are indicated by arrows.

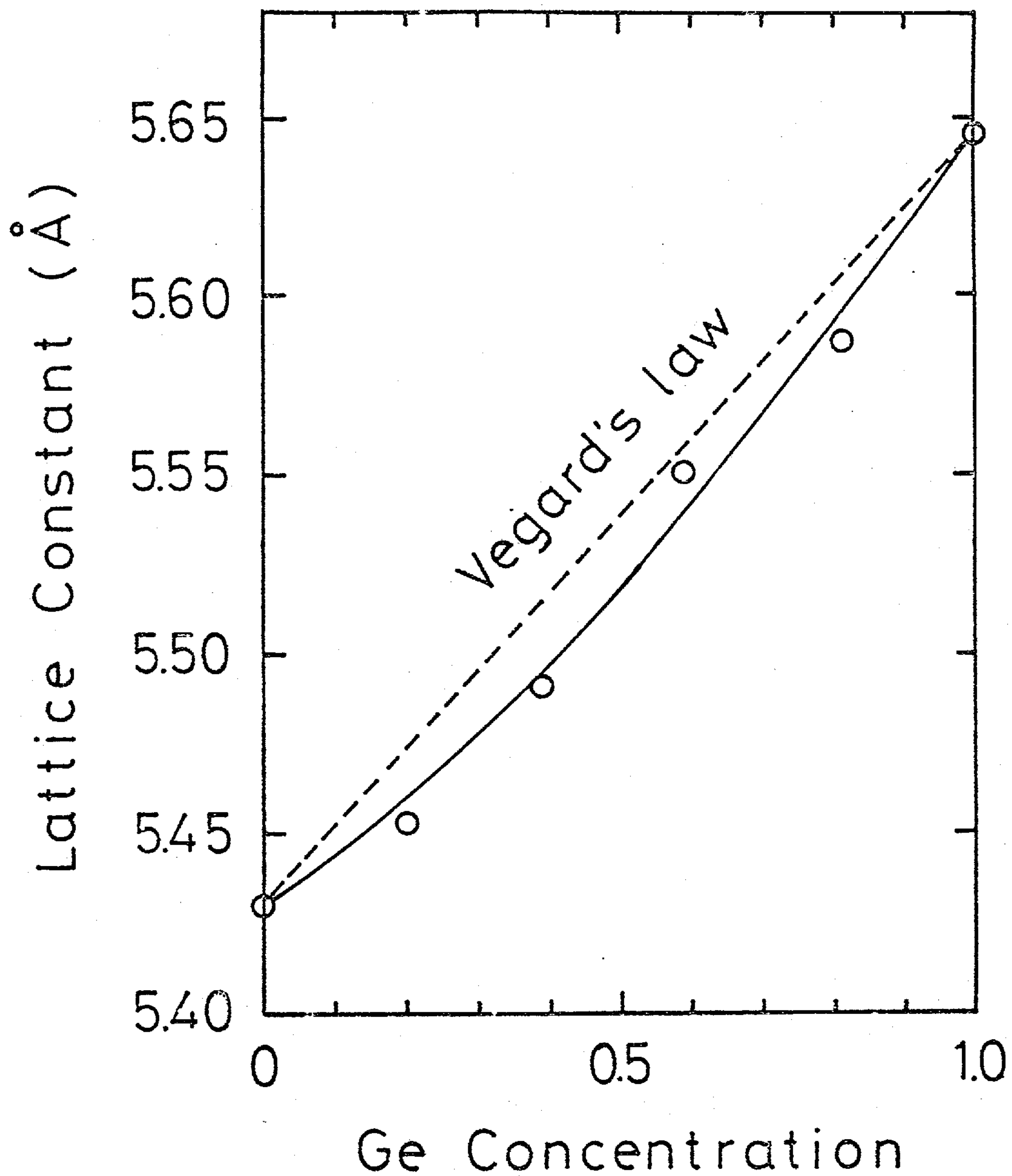

Fig.23 Dependence of lattice constant of crystalline $Si_{1-x}Ge_x$ alloys on composition determined by x-ray diffraction measurement is shown by the solid line. The dashed line represents Vegard's law.

5. CONCLUSIONS

EXAFS (extended X-ray absorption fine structure) is a powerful probe to study local structure around the atom of the specific element. In conventional EXAFS analyses, it has been known that reliable structures are obtained with different values of absorption edge energy, E_0, for different neighboring atoms. It is shown in this study that the Ge- K edge EXAFS resulting from the Ge-Ge and Ge-Si bonds in hydrogenated amorphous Si-Ge alloys can be excellently explained by a unique E_0 value provided that a newly developed formula based on the spherical wave functions of photoelectrons is used.

The microscopic structures of hydrogenated amorphous silicon-germanium alloys and crystalline silicon-germanium alloys have been determined using the EXAFS method. In a-$Si_{1-x}Ge_x$:H, it has been shown that Ge-Ge and Ge-Si bond lengths are constant throughout the entire compositional range and equal to 2.46Å and 2.41Å, respectively. The Ge-Si bond length is found to be close to the average value of the bond lengths for both Ge and Si crystals. A study of the coordination around Ge atoms has revealed that Ge and Si atoms are randomly mixed in the Ge concentration range below 40 atomic percent. In films with high Ge content, the coordination of Ge atoms is 15-20 percent higher than that expected for a random mixture of Ge and Si atoms, suggesting a structural inhomogeneity in Ge-rich alloys.

In crystalline silicon-germanium alloys, it has been shown that bonds relax completely, while lattice constant varies monotonously with composition. Significant changes in bond

length with Ge composition from 0.2 to 0.8 are not detected; 2.45Å for Ge-Ge bond and 2.40Å for Ge-Si bond. A study of coordination around Ge atoms has shown that atoms are randomly mixed in the range of Ge concentration studied. These results support the Bragg's and Pauling's notion that says the bond lengths in alloys are the sum of the atomic radii, hence they are independent on compositions.

6. ACKNOWLEDGEMENTS

The author would like to acknowledge Dr. A. Fukuhara of Advanced Reserach Laboratory, Hitachi, Ltd., for valuable discussions and continuous stimulation throughout this work. He is also grateful to Drs. S. Muramatsu and T. Shimada of Central Research Laboratory, Hitachi, Ltd., and Dr. Y. Nishino of Nagoya Institute of Technology for experiments and useful discussions. Thanks are due to Drs. K. Hayakawa and E. Maruyama of Advanced Research Laboratory, Hitachi, Ltd., for giving me the opportunity to conduct this work. Finally, he expresses his gratitude to Prof. T. Ohta of Hiroshima University for being interested in this work and critical reading of the manuscript.

REFERENCES

1. H. Fricke, Phys. Rev. 16, 202 (1920).
2. Reviews on fundamentals of EXAFS spectroscopy and its capplication to structural study is described in detail by T. M. Hayes and J. B. Boyce in Solid State Physics, Vol37, 173 (1983).
3. See, for example, Synchrotron Radiation Research, edited by H. Winick and S. Doniach (Plenum, New York, 1980).
4. D. E. Sayers, E. A. Stern and F. W. Lytle, Phys. Rev. Lett. 27, 1204 (1971).
5. S. P. Cramer K. O. Hodgson, E. I. Stiefel and W. E. Newton, J. Am. Chem. Soc,100, 2748 (1978).
6. B.- K. Teo, R. G. Shulman, G. S. Brown and A. E. Meixner, J. Am. Chem. Soc. 101, 5624 (1979).
7. B.- K. Teo, M. R. Antonio and B. A. Averill, J. Am. Chem. Soc, 105, 3751 (1983).
8. S. Muramatsu, S. Kokunai, Y. Nishino, H. Kajiyama, S. Matsubara, H. Itoh, N. Nakamura and T. Shimada, accpeted for publication, Applied Surface Science.
9. H. Oyanagi, T. Matsushita, M. Ito and H. Kuroda, KEK Report, KEK83-30 (1984).
10 Y. Hirai, KEK Report, KEK85-1, 57 (1986).
11. The absorption edge energy thus determined has been shown to provide the best-fit in the analysis of a-Ge:H (Ref.15). The edge energy for a-$Si_{1-x}Ge_x$:H was determined in the same way.
12. M. Nomura, K. Asakura, U. Kaminaga, T. Matsushita,K. Kohra, and H. Kuroda, Bull. Chem. Soc. Jpn. 55, 3911 (1982).

13. W. L. Schaich, Phys. Rev. B29, 6513 (1984).

14. S. J. Gurman, N. Binstead and I. Ross, J. Phys. C17, 143 (1984).

15. A. Fukuhara and H. Kajiyama, in preparation for publication.

16. P. A. Lee and J. B. Pendry, Phys. Rev. B11, 2795 (1975).

17. B.- K. Teo and P. A. Lee, J. Am. Chem. Soc. 101, 2815 (1979).

18. F. Herman and S. Skillman,in Atomic Structure Calculations (Prentice-Hall, Englewood Cliffs, N. J., 1963).

19. J. B. Pendry, J. Phys. C4, 2501 (1971); C5, 2567 (1972); the program is listed in Low Energy Electron Diffraction by J. B. Pendry (Academic, New York, 1974).

20. International Tables for X-Ray Crystallography III, edited by K. Lansdale et al., (Kyonoch, Birmingham, 1962).

21. American Institute of Physics Handbook, 3rd ed. (McGraw-Hill, New York, 1972).

22. H. Gant and W. Monch, Sur. Sci. 105, 217 (1981).

23. Morimoto, T. Miura, M. Kumeda and T. Shimizu, Jpn. J. Appl. Phys. 20, L833 (1981).

24. S. Minomura, K. Tsuji, M. Wakagi, T. Ishidate, K. Inoue and M. Shibuya, J. Non-cryst. Solids 58-60, 541 (1983).

25. L. Incoccia, S. Mobilio, M. G. Proietti, F. Fiorini, C. Giovannela and F. Evangelisti, Phys. Rev. B31, 1028 (1985).

26. G.Nakamura, K. Sato, T. Ishihara, M. Usui, H. Sasaki, K. Okaniwa and Y. Yukimoto, in Proceedings of the 1st International Photovoltanic Science and Engineering Conference (Kobe, Japan, 1984), p.578

27. J. Yang, T. Glatfeiter, J. Burdick, J. P. Fourier, L. Bomem, R. Ross and R. Mohr, in Proceedings of the 2nd International Photovoltaic Science and Engineering Conference (Beijing, China, 1986), p.361.

28. K. D. Mackenzie, J. R. Eggert, D. J. Leopold, Y. M. Li, S. Lim and W. Paul, Phys. Rev. B31, 2198 (1985).

29. R. J. Temkin, G. A. N. Cornell and W. Paul, Solid State Commun. 11, 1591 (1978).

30. Y. Nishino and Y. Takano, Jpn. J. Appl. Phys. 25, 885 (1986).

31. G. Lucovsky, R. J. Nemanich, and J. C. Knights, Phys. Rev. B19, 2064 (1979).

32. J. P. Dismukes, L. Ekstrom and R. J. Paff, J. Phys. Chem, 68, 3021 (1964).

33. E. R. Jhonson and S. M Christian, Phys. Rev. Lett, 560 (1954).

34. J. L. Martin and A. Zunger, Phys. Rev. B30, 6217 (1984).

35. T. Ito , Jpn. J. Appl. Phys, 26, 256 (1987).

36. Huang, Proc. R. Soc. London, Ser. A190, 102 (1947).

37. W. L. Bragg, Philos. Mag. 40, 169 (1920).

38. L. Pauling and M. L. Hugins, Z. Kristallogr. Kristallgeom. Kristallphys. Kristallchem. 87, 205 (1934).

39. L. Vegard, Z. Phys. 5, 17 (1921).

40. P. N. Keating, Phys. Rev. 145, 637 (1966).

41. C. V. Fong, W. Weber and J. C. Philips, Phys. Rev. B12, 5387 (1976).

42. J. C. Mikekelson, Jr and J. B. Boyce, Phys. Rev. Lett. 49, 1412 (1982).

43. T. Sasaki, T. Onoda, R. Ito, and N. Ogasawara, Jpn. J. Appl. Phys. 25, 231 (1986).

44. A. Fontaine, P. Lagarde, A. Naudon, D. Raoux, and D. Sapanjarrd, Philos. Mag. B4, 17 (1979).

45. B. Lengeler and P. Wisenberger, Phys. Rev. B21, 4507 (1980).